

Original Article

hsa_circ_0000519 promotes the progression of lung adenocarcinoma through the hsa-miR-1296-5p/DARS axis

Guangxu Tu^{1,2}, Weilin Peng^{1,2}, Xiong Peng^{1,2}, Zhenyu Zhao^{1,2}, Shuai Shi^{1,2}, Qidong Cai^{1,2}, Boxue He^{1,2}, Wei Yin^{1,2}, Shaoliang Peng^{3,4}, Li Wang^{1,2}, Fenglei Yu^{1,2}, Xiang Wang^{1,2}

¹Department of Thoracic Surgery, The Second Xiangya Hospital, Central South University, Changsha 410011, Hunan, China; ²Hunan Key Laboratory of Early Diagnosis and Precision Therapy, The Second Xiangya Hospital, Central South University, Changsha 410011, Hunan, China; ³College of Computer Science and Electronic Engineering, Hunan University, Changsha 410082, Hunan, China; ⁴School of Computer Science, National University of Defense Technology, Changsha 410073, Hunan, China

Received May 24, 2023; Accepted July 18, 2023; Epub August 15, 2023; Published August 30, 2023

Abstract: Emerging research indicates that circRNAs serve a crucial role in occurrence and development of cancers. This study aimed to uncover the biological role of hsa_circ_0000519 in the progression of LUAD (lung adenocarcinoma). hsa_circ_0000519 was identified by bioinformatic analysis, and its differential expression was validated in LUAD tissues and cell lines. CCK8, colony formation, wound healing, transwell assays, and xenograft tumor models were used to observe the biological functions of hsa_circ_0000519. FISH, RIP, dual luciferase reporter assays, and recovery experiments were implemented to explore the underlying mechanisms of hsa_circ_0000519. hsa_circ_0000519 was significantly upregulated in LUAD tissues and cell lines. The expression of hsa_circ_0000519 was positively correlated with T grade and TNM stage in patients with LUAD. Downregulation of hsa_circ_0000519 remarkably reduced cell proliferation, migration, invasion in vitro, and tumor growth in vivo. Mechanistic investigation demonstrated that hsa_circ_0000519 directly sponged hsa-miR-1296-5p to reduce its repressive impact on DARS as well as activate the PI3K/AKT/mTOR signaling pathway. The malignant phenotypes of LUAD cells induced by upregulation of hsa_circ_0000519 could be rescued by hsa-miR-1296-5p overexpression or knockdown of DARS. In conclusion, hsa_circ_0000519 promotes LUAD progression through the hsa-miR-1296-5p/DARS axis and may be expected as a novel biomarker and therapeutic for LUAD.

Keywords: LUAD, hsa_circ_0000519, hsa-miR-1296-5p, DARS, ceRNA, PI3K/AKT/mTOR pathway

Introduction

Lung cancer (LC) is one of the most frequent types of malignant tumors, and it is also one of the deadliest [1-3]. LC is divided into two pathologic types: small cell lung cancer (SCLC) and non-small cell lung cancer (NSCLC), with about 85% of cases being NSCLC [3, 4]. Despite substantial advances in diagnosis and treatment (e.g., surgical modalities, targeted therapies, and immunotherapy), the prognosis of NSCLC patients remains far from satisfactory [4, 5]. As the most common subtype of NSCLC, LUAD (lung adenocarcinoma) accounts for approximately 40% of all LC cases [6]. Unfortunately, the 5-year overall survival rate of LUAD patients

is as low as 21% [7]. In order to develop novel biomarkers and effective therapeutic targets, it is crucial to explore new molecular targets along with their mechanisms in the occurrence and development of LUAD.

Non-coding RNA (ncRNA), which consists of microRNAs (miRNAs), long non-coding RNAs (lncRNAs), etc., makes up more than 90% of all human transcripts [8, 9]. Emerging research indicated that endogenous circular RNAs (circRNAs) play an important role in the transcriptional and post-transcriptional control of gene expression [10]. CircRNAs, a novel type of endogenous non-coding RNA, are less susceptible to exonuclease degradation due to their

closed circular structure, making them an ideal candidate for cancer diagnosis and treatment [11-13]. Recent research suggested that circRNA dysregulation may be linked to NSCLC proliferation, metastasis, drug resistance, and immune escape. For example, as a miRNA sponge, circSATB2 upregulated the expression of FSCN1, which increased cell proliferation, migration, and invasion [14]. In addition, NSCLC tissues highly expressed circ-HSP90A. Cell proliferation, migration, invasion, and the ability to evade immune surveillance were all drastically reduced with circ-HSP90A knockdown. Mechanically, by competitively absorbing miR-424-5p, circ-HSP90A increased the expression of PD-L1 [15]. However, a complete understanding of circRNA's function and mechanism in LUAD is still lacking.

MicroRNAs were found to be implicated in a variety of NSCLC phenotypes, including proliferation, epithelium-mesenchymal transition, and drug resistance [16-20]. By binding to their complementary sequences in the 3'UTR of mRNAs, miRNAs exert their functions as post-transcriptional regulators [21]. Interestingly, by binding to the miRNA response elements (MREs), circRNAs could mitigate the silencing effects of miRNAs. For example, through a direct interaction with hsa-miR-200b-3p, hsa_circ_103820 inhibited NSCLC cell proliferation, motility, and invasion through the regulation of hsa-miR-200b-3p's downstream substrates LATS2 and SOCS6 [22]. In NSCLC tissues and cell lines, circFBX07 was downregulated, while overexpression of circFBX07 inhibited NSCLC cell proliferation by absorbing miR-296-3p and raising KLF15 expression, consequently transactivating CDKN1A expression [23].

Aspartyl-tRNA synthetase (DARS), a member of the aminoacyl tRNA synthetases (ARSs) family, is responsible for the ligation of aspartate to corresponding aspartate tRNAs, providing crude materials for protein synthesis, and ensuring translation fidelity [24]. High levels of DARS expression in gastric cancer have been linked to advanced clinicopathological stages and shorter overall survival times in previous research. Functionally, downregulation of DARS significantly inhibited gastric cancer cell proliferation [25]. In addition, Min Jiao et al. found that clear cell renal carcinomas highly expressed the lncRNA DARS-AS1. DARS-AS1 upregulation was reported to boost clear cell

renal carcinoma cell proliferation by competitive sponging of miR-194-5p and increased DARS expression. Furthermore, DARS knockdown greatly suppressed cell growth, suggesting that it functions as an oncogene [26]. However, research on the expression and biological role of DARS in LUAD is still blank.

The I3K/AKT/mTOR signaling pathway is considered to be one of the most common signaling pathways in human cancers [27], including LUAD. For example, the upregulation of the lncRNA CCAT1 could enhance the proliferation and angiogenesis of LUAD cells by mediating the translocation of fatty acid binding protein 5 (FABP5) into the nucleus and activating the PI3K/AKT/mTOR signaling pathway [28]. Fangyuan Yu et al. reported that SLITRK6 was significantly upregulated in LUAD tissues, and knockdown of SLITRK6 substantially inhibited the proliferation and glycolysis of LUAD cells by inactivating the PI3K/AKT/mTOR signaling pathway [29]. In addition, ADAM metallopeptidase domain 12 (ADAM12) was reported to be significantly increased in LUAD tissues and correlated with poor prognosis of LUAD patients [30]. Besides, overexpression of ADAM12 accelerated the proliferation, apoptosis escape, invasion and migration, angiogenesis, immune escape and EGFR-TKI resistance by activating the PI3K/Akt/mTOR and RAS signaling pathways. However, few studies have reported the regulatory effect of circRNAs on the PI3K/AKT/mTOR signaling pathway in LUAD.

In the present study, we determined a LUAD-associated circRNA hsa_circ_0000519 by bioinformatics. The upregulation of hsa_circ_0000519 was correlated with a more advanced T grade and TNM stage of LUAD patients. As a ceRNA for hsa-miR-1296-5p, hsa_circ_0000519 could promote LUAD progression by forcing DARS expression and activating the PI3K/AKT/mTOR signaling pathway. The findings of this study further expanded the research on the significance of circRNAs in LUAD progression and may bring new insights for the exploitation of novel biomarkers and therapeutics for LUAD.

Material and methods

LUAD tissue samples and cell lines

From 2021 to 2022, a total of 48 matched LUAD tissues and non-tumoral lung tissues

were obtained from patients who received radical excision of LUAD at the Second Xiangya Hospital of Central South University. All tissues were frozen in liquid nitrogen until RNA was extracted. The American Joint Committee on Cancer (AJCC) Classification, Eighth Edition, was used to validate the pathological diagnosis. The research was approved by the Ethics Committee of the Second Xiangya Hospital, Central South University (202103-148) and informed consent was obtained from all participants involved in the study.

A549, H1299, H358, PC9, and SPC-A1 LUAD cell lines, together with the BEAS-2B normal bronchial epithelial cell line, were obtained from the Chinese Academy of Science Cell Bank (Shanghai, China). While DMEM/F-12 (Gibco, USA) was used to take care of A549 cells, RPMI-1640 (Gibco, USA) was used for BEAS-2B, H1299, H358, PC9, and SPC-A1 cells. Both mediums were supplemented with 10% fetal bovine serum (FBS) (Gibco, USA) and 1% penicillin-streptomycin resolution (Gibco, USA).

Bioinformatics analysis

To screen out the differentially expressed circRNAs in NSCLC, bioinformatic analyses were performed on three circRNA microarray datasets, namely GSE101586 [31], GSE101684 [32] and GSE158695 [33], which were determined by the search keywords of (“lung cancer”) AND (“tissue”) AND (“circRNA” or “circular RNA”) in the GEO database (Gene Expression Omnibus). The GSE101586, GSE101684, and GSE158695 datasets consisted of circRNA microarray expression profiles from 5 LUAD patients, 4 LUAD patients, and 3 NSCLC patients, respectively.

MiRNAs sharing binding sites with hsa_circ_0000519 were predicted in CircInteractome (<https://circinteractome.nia.nih.gov/index.html>) [34], CircBank (<http://www.circbank.cn/index.html>) [35], and ENCORI (<https://starbase.sysu.edu.cn/index.php>) [36]. ENCORI (same as aforementioned), TargetScan (https://www.targetscan.org/vert_80/) [37], and TarBase (<https://dianalab.e-ce.uth.gr/html/diana/web/index.php?r=tarbasev8%2Findex>) [38] were used to analyze hsa-miR-1296-5p's target genes. Clinical and RNA-seq data for LUAD patients were obtained from the TCGA data-

base. The “Limma” and “Survival” R packages were used for the differentially expressed analysis of DARS in LUAD and investigating the connection between DARS expression and the prognosis in LUAD patients, respectively. Utilizing GSEA 4.0.2, signaling pathways associated with DARS dysregulation were identified by Gene Set Enrichment Analysis (GSEA).

RNA extraction and RT-qPCR

Using TRIzol (Invitrogen, USA), total RNA from LUAD tissues, normal lung tissues, and LUAD cell lines was extracted. A Genomic DNA kit (CWBI, China) was used to extract gDNA according to the protocol. The concentrations and purities of RNAs were evaluated using a Nanodrop 2000 (Thermo Fisher Scientific, USA). CircRNAs and mRNAs were reversely transcribed using the 1st Strand cDNA Synthesis SuperMix (YEASEN, China). MiRNA First Strand cDNA Synthesis Kit (Sangon Biotech, China) with stem-loop primers was used for reverse transcription. mRNA transcripts were quantified using an ABI StepOne sequence detection system (Applied Biosystems, USA) and a qPCR SYBR Green Master Mix (YEASEN, China). We performed these steps three times for each sample, using GAPDH and U6 as internal standards. We compared the expression of circRNAs, miRNAs, and mRNAs to an internal standard using the $2^{-\Delta\Delta CT}$ method. In this investigation, hsa_circ_0000519 was amplified by divergent primers, while liner mRNA was amplified by convergent primers. The primers were displayed in [Supplementary Table 1](#).

Nucleic acid electrophoresis

cDNA and gDNA PCR products were separated by electrophoresis on a 2% agarose gel with the use of TAE running buffer at 100 V for 30 minutes using a Marker L in the size range of 50 to 500 bp (Sango Biotech, China). ChemiDoc XRS+ imaging equipment (BIO-RAD, USA) was employed to spot the DNA bands.

Fluorescence in situ hybridization (FISH)

Probes of Cy3-labeled hsa_circ_0000519 (RI-OBO, China) were developed for FISH tests to identify the natural hsa_circ_0000519 localization in A549 and PC9 cells. Images were obtained using an Olympus BX63 fluorescent

hsa_circ_0000519 promotes lung adenocarcinoma progression

microscope (Olympus, Japan) after the probes had been hybridized using the kit's specified procedures (RIOBO, China).

Isolation of cytoplasmic and nuclear RNA

Briefly, 1×10^7 cells were resuspended in 1 ml of cold PBS. To begin total RNA extraction, we mixed 200 μ l of resuspended cells with 800 μ l of RNAiso Plus reagent (Takara, Japan). After centrifuging the residual suspensions at 1000 rpm for 5 minutes, they were resuspended in 200 μ l of TD buffer containing 1% NP40. After separating the cells into two layers through centrifugation at 5000 rpm for 30 seconds, cytoplasmic RNA was extracted by aspirating the supernatant into 800 μ l of RNAiso Plus reagent. The nuclear RNA was extracted by resuspending the precipitates in 200 μ l of cold TD buffer containing 0.5% NP40 and then treating them with 800 μ l of RNAiso Plus reagent. Subcellular localization of hsa_circ_0000519 was determined by reverse transcription and RT-qPCR of total RNA, cytoplasmic RNA, and nuclear RNA.

RNA immunoprecipitation (RIP)

Following the protocol provided by the manufacturer of the RIP kit (Genesee Biotech, China), RIP experiments were conducted on A549 and PC9 cells. To summarize, 1×10^7 cells were lysed and treated with anti-AGO2 or anti-IgG antibody-coated magnetic beads overnight at 4°C. After RNA was rinsed from the magnetic beads, reverse transcription and RT-qPCR detection were performed.

Dual luciferase reporter assays

This study used the Dual Luciferase Reporter Gene Assay Kit (YEASEN, China). Subcloning sequences of hsa_circ_0000519 and DARS 3'UTR into the pmir-GLO (Promega, USA) empty vector yielded the wild-type dual luciferase plasmids hsa_circ_0000519-WT and DARS 3'UTR-WT, respectively. We created hsa_circ_0000519-MUT and DARS 3'UTR-MUT dual luciferase plasmids with mutated sequences that may bind to hsa-miR-1296-5p. Co-transfection of hsa-miR-1296-5p mimics or inhibitor with the dual luciferase plasmids was performed in the A549 and PC9 cell lines. A Dual-Luciferase Reporter Assay System (Promega, USA) was then employed to detect the relative activities of luciferase.

Vector construction and stable transfection

Tsingke Biotech (Changsha, China) was contacted to acquire the shRNAs (referred to as sh-circ 1-3#, [Supplementary Table 2](#)) aimed at the back-splicing junction of hsa_circ_0000519. To make the overexpression plasmid (termed oe-circ), we inserted the whole hsa_circ_0000519 cDNA into the PLC5-ciR (Gene-seed Biotech, China) empty vector. In the A549 and PC9 cells, stable transfections were done using empty vectors serving as negative controls, as previously described [39].

Transient transfection

In a 6-well plate, cells were seeded until cell confluency reached 50%-60%. Transient expression of si-DARS (Tsingke Biotech, China), oe-DARS (VectorBuilder, China), and mimics as well as inhibitor of hsa-miR-1296-5p (Sango Biotech, China) in A549 or PC9 cells was achieved by Lipofectamine 3000 (Invitrogen, USA).

Western blot

RIPA (Beyond, China) was used to lyse the cells. The bicinchoninic acid (BCA) reagent (Beyond, China) was implemented to ascertain the amounts of proteins. After that, proteins were transferred to PVDF membranes (Millipore, USA) using 10% SDS-PAGE. Antibodies against DARS (1:20000, Proteintech, USA), GAPDH (1:10000, Proteintech, USA), AKT (1:2000, Servicebio, China), phospho-AKT (1:1000, Zen-BioScience, China), mTOR (1:1000, Servicebio, China), or phospho-mTOR (1:1000, Servicebio, China) were then incubated with the PVDF membranes at 4°C overnight. Protein bands were detected using Super ECL Prime (Everbright, USA) after PVDF membranes were incubated with the secondary antibody (1:2000, CST, USA) for 1 hour at room temperature.

Immunohistochemistry (IHC)

For IHC, the HRP-Polymer IHC Kit (AiFang Biological, China) was used. The subcutaneous tumor tissues of nude mice were paraffin-embedded, paraformaldehyde-fixed, and sectioned. Tumor tissue sections were first treated with an anti-Ki-67 primary antibody at 4°C overnight, after which they were incubated with an HRP-conjugated secondary antibody for 30 minutes. Sections were stained with DAB and

hsa_circ_0000519 promotes lung adenocarcinoma progression

hematoxylin after being rinsed three times in PBST for microscopic photography.

CCK8 and colony formation

The CCK-8 and colony formation tests were used to measure cells' capacity for proliferation. One thousand cells were seeded into 96-well plates for CCK-8 tests. At 0, 24, 48, 72, and 96 hours, 10 μ l of CCK-8 reagents were dropped to the 96 plates. After 2 hours of incubation at 37°C, the absorbance at 450 nm was detected with an infinite M200 spectrophotometer (Tecan, Switzerland). A colony formation experiment was performed by growing 1,000 treated cells in six-well plates at 37°C and 5% CO₂ until colonies formed. Cell colonies were stained with a 0.5% crystal violet solution for 15 minutes after being fixed in 4% paraformaldehyde. Colony counts were taken from photographs of air-dried 6-well plates. There were three separate runs of each experiment.

Wound healing assays

Scratched wounds were made in LUAD cells by scraping the end of a 200 μ l pipette over the surface of the cells after they had been seeded into six-well plates and grown at 37°C in a 5% CO₂ incubator until cell confluency reached roughly 80%-90%. After further cultivating the LUAD cells in the matching serum-free mediums, scratch wound closure was photographed at 0 and 24 hours. The proportion of wound closure was determined by determining the percentage by which the scratch distance between cells was reduced after 24 hours compared to before. The experiment was performed three times by each of the groups.

Transwell assays

Transwell invasion and migration experiments, employing chambers (Corning, USA) covered with or without Matrigel (BD Biosciences, USA) on the upper face of the membrane, were used to assess LUAD cell invasion and migration. The top chamber, where 4 \times 10⁴ cells in 200 μ l of serum-free medium were settled, was transferred to a 24-well plate with 600 μ l of matching complete medium and cultured for 24 hours. The cells on the inferior face of the chamber membrane were stained with 0.5% crystal violet for 15 minutes after being fixed in 4% paraformaldehyde, while the unigrated

cells on the upper face of the chamber membrane were cleaned off with a cotton swab. After air drying the chambers, photographs of five randomly selected fields were taken. This procedure was performed three times.

Xenograft tumor models in nude mice

Animal experiments were approved by the Animal Ethical and Welfare Committee of the Second Xiangya Hospital, Central South University (202205-376) and conducted in accordance with the guidelines of the National Health Institute. Four-week-old female BALB/c nude mice were obtained from Hunan SJA Laboratory Animal Co., Ltd. (Hunan, China). Five million A549 or PC9 cells (stably transfected with vector/oe-circ or sh-Ctrl/sh-circ 1#) in 100 μ l PBS were injected subcutaneously into the right back of each animal. Every four days, xenograft tumors were measured for their length (L) and width (W), and subcutaneous tumor volumes were determined by the formula Volume = L \times W²/2. Mice were euthanized after 28 days, and the xenograft tumors were weighed and then subjected to RT-qPCR and IHC.

Statistical analysis

The GraphPad Prism v9.0.0 software was used for statistical analyses. The paired or unpaired t-test was used for the comparison of quantitative variables, and the chi-square test for qualitative variables. Pearson correlation analysis was used to analyze the expression correlation between hsa_circ_0000519, hsa-miR-1296-5p, and DARS. P<0.05 was considered statistically significant and represented by * (P<0.05), ** (P<0.01), *** (P<0.001), and **** (P<0.0001). The threshold for screening differentially expressed circRNAs in the GEO database was set as P<0.05 and |log₂(FC)| \geq 1. Signaling pathways with a normalized P<0.05, |NES|>1 and FDR-q value <0.25 were considered significantly enriched in the GSEA.

Results

Expression profiles of hsa_circ_0000519 in LUAD tissues and cell lines

We performed bioinformatic analyses of three circRNA-sequencing datasets (GEO accession numbers GSE101586, GSE101684, and GSE-

hsa_circ_0000519 promotes lung adenocarcinoma progression

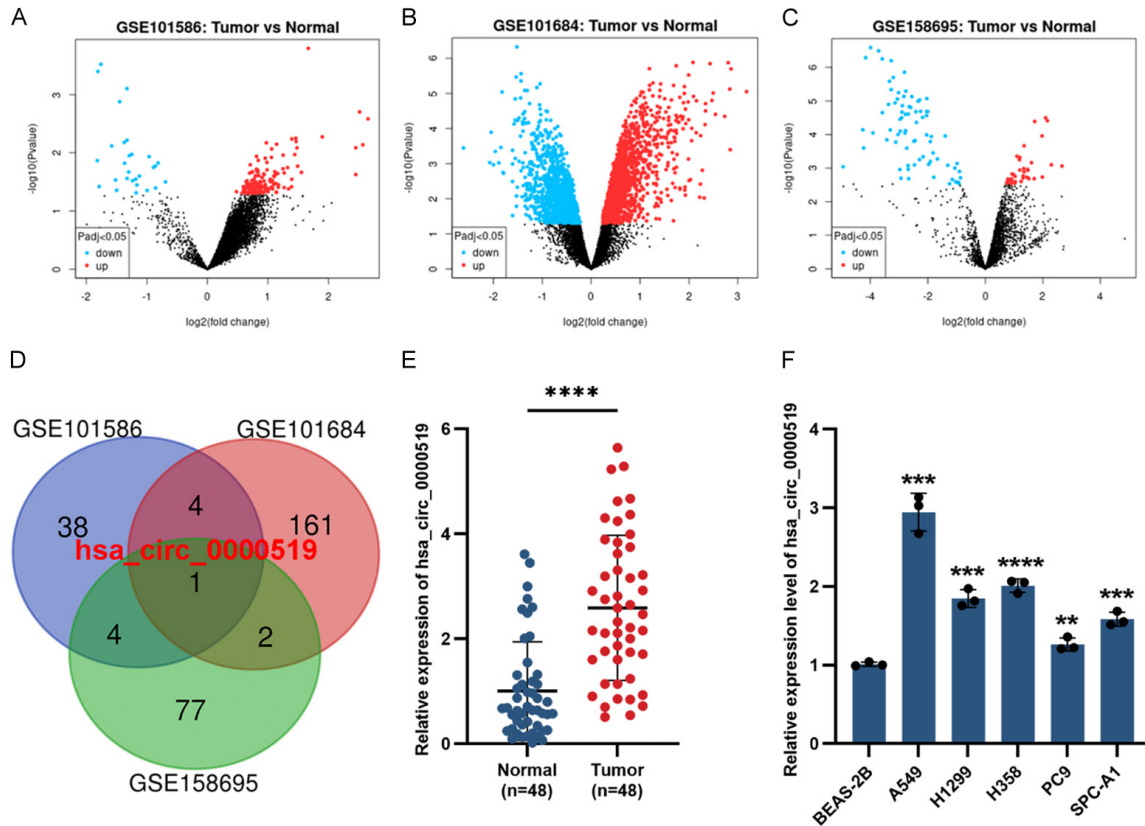


Figure 1. The expression level of hsa_circ_0000519 is elevated in LUAD tissues and cell lines. A-C. Differentially expressed genes in the GSE101586, GSE101684, and GSE158695 datasets were visualized by volcano plots. D. By overlapping the up-regulated circRNAs across three datasets, hsa_circ_0000519 was identified. E. Verification of hsa_circ_0000519 expression in 48 LUAD specimens and their matching normal lung tissues. F. The expression of hsa_circ_0000519 was analyzed in LUAD cell lines.

158695) to investigate the potential contribution of dysregulated circRNAs to LUAD progression. Differentially expressed circRNAs were identified in these datasets (as shown **Figure 1A-C** and **Supplementary Tables 3, 4, 5**) using the filter parameters of $P < 0.05$ and $\log_2|FC| \geq 1$. By overlapping the elevated circRNAs, we discovered that only hsa_circ_0000519 showed consistently high expression in all three datasets (**Figure 1D**). Thus, hsa_circ_0000519 was chosen for further analysis. Afterwards, hsa_circ_0000519 was validated to be markedly upregulated in 48 LUAD tissues by RT-qPCR (**Figure 1E**). In addition, there was a positive correlation between hsa_circ_0000519 expression and LUAD patients' T grade and TNM stage (**Table 1**). The expression of hsa_circ_0000519 was then analyzed in LUAD cell lines. As shown in **Figure 1F**, A549 and PC9 cell lines had the highest and lowest expressions of hsa_circ_0000519, respective-

ly. Therefore, A549 and PC9 cell lines were used to investigate the downstream mechanism of hsa_circ_0000519.

Characterization of hsa_circ_0000519

hsa_circ_0000519 is formed by the head-to-tail splicing of a 98-bp pre-mRNA (from 20811436 to 20811534) from its host gene RPPH1 on chromosome 14 (**Figure 2A**). To confirm that the head-to-tail splicing of hsa_circ_0000519 was generated by trans-splicing rather than genomic rearrangement of RPPH1, cDNA as well as gDNA from A549 and PC9 cell lines were amplified with convergent primers and divergent primers, respectively, and then run on an agarose gel electrophoresis. As shown in **Figure 2B**, hsa_circ_0000519 was exclusively discovered in the cDNA of A549 and PC9 cell lines. To ascertain the stability of hsa_circ_0000519, total RNA from A549 and PC9 cell lines was treated with or without RNase R

Table 1. Correlation between hsa_circ_0000519 expression and clinicopathologic characteristics in 48 individuals with LUAD

Characteristics	Case	hsa_circ_0000519 expression		p value
		Low	High	
All cases	48	8	40	
Age at surgery (years)				0.676
<60	33	6	27	
≥60	15	2	13	
Gender				0.696
Male	21	3	18	
Female	27	5	22	
T grade				0.02
T1+T2	24	7	17	
T3+T4	24	1	23	
Lymph node invasion				0.282
Negative (N0)	37	5	32	
Positive (N1-N3)	11	3	8	
TNM stage				0.014
I-II	23	7	16	
III-IV	25	1	24	

and subjected to RT-qPCR. As a result, hsa_circ_0000519 showed an extremely high resistance to RNase R digestion, suggesting the presence of a loop structure (Figure 2C, 2D). FISH assays indicated that hsa_circ_0000519 was primarily located in the cytoplasm (Figure 2E), which was further validated by RT-qPCR analyses of isolated cytoplasmic and nuclear RNA in A549 and PC9 cell lines (Figure 2F, 2G), indicating that hsa_circ_0000519 may have a role in post-transcriptional regulation.

hsa_circ_0000519 promotes LUAD cell proliferation, migration, and invasion in vitro

To achieve reproducible overexpression or knockdown of hsa_circ_0000519, hsa_circ_0000519 overexpression vector (referred to as oe-circ) and three shRNAs against the back-splicing sites were stably transfected into LUAD cell lines. The oe-circ vector was stably transfected into PC9 and SPC-A1 cell lines, as it evidently increased the expression level of hsa_circ_0000519 instead of RPPH1 mRNA (Figure 3A, 3B). Among the three shRNAs against hsa_circ_0000519, sh-circ 1# and 2# showed satisfactory inhibition efficiencies (Figure 3C), which were used for further investigations.

Then, CCK8 and colony formation assays were carried out to evaluate proliferative capabilities of LUAD cell lines. CCK8 assays showed that upregulation of hsa_circ_0000519 substantially enhanced the proliferation of PC9 and SPC-A1 cell lines, while downregulation of hsa_circ_0000519 in the A549 cell line reduced this effect (Figure 3D). Similar results were found in colony formation experiments (Figure 3E), where upregulation of hsa_circ_0000519 considerably boosted colony formation capabilities while knockdown of hsa_circ_0000519 decreased these abilities. According to these results, hsa_circ_0000519 accelerated the growth of LUAD cells.

hsa_circ_0000519's influence on LUAD cell migration and invasion was assessed by wound healing and transwell assays. Migration and invasion abilities were significantly improved by overexpression of hsa_circ_0000519 but dramatically reduced by knockdown of hsa_circ_0000519 (Figure 3F, 3G). These findings indicated that hsa_circ_0000519 promoted LUAD cell migration and invasion.

hsa_circ_0000519 promotes LUAD tumor proliferation in vivo

PC9-vector/oe-circ and A549-sh-Ctrl/sh-circ 1# were subcutaneously injected into BALB/c nude mice to further evaluate the impact of hsa_circ_0000519 on tumor growth. Results showed that tumor volume and weight in the oe-circ group were substantially higher than those in the vector group. In contrast, knockdown of hsa_circ_0000519 exhibited the opposite tendency (Figure 4A-C). The tumor tissues were then analyzed by RT-qPCR and immunohistochemistry. A significant upregulation of hsa_circ_0000519 was determined in the oe-circ group, while the hsa_circ_0000519 knockdown group was just the opposite (Figure 4D, 4E). In addition, IHC results revealed that Ki-67 expression was evidently

hsa_circ_0000519 promotes lung adenocarcinoma progression

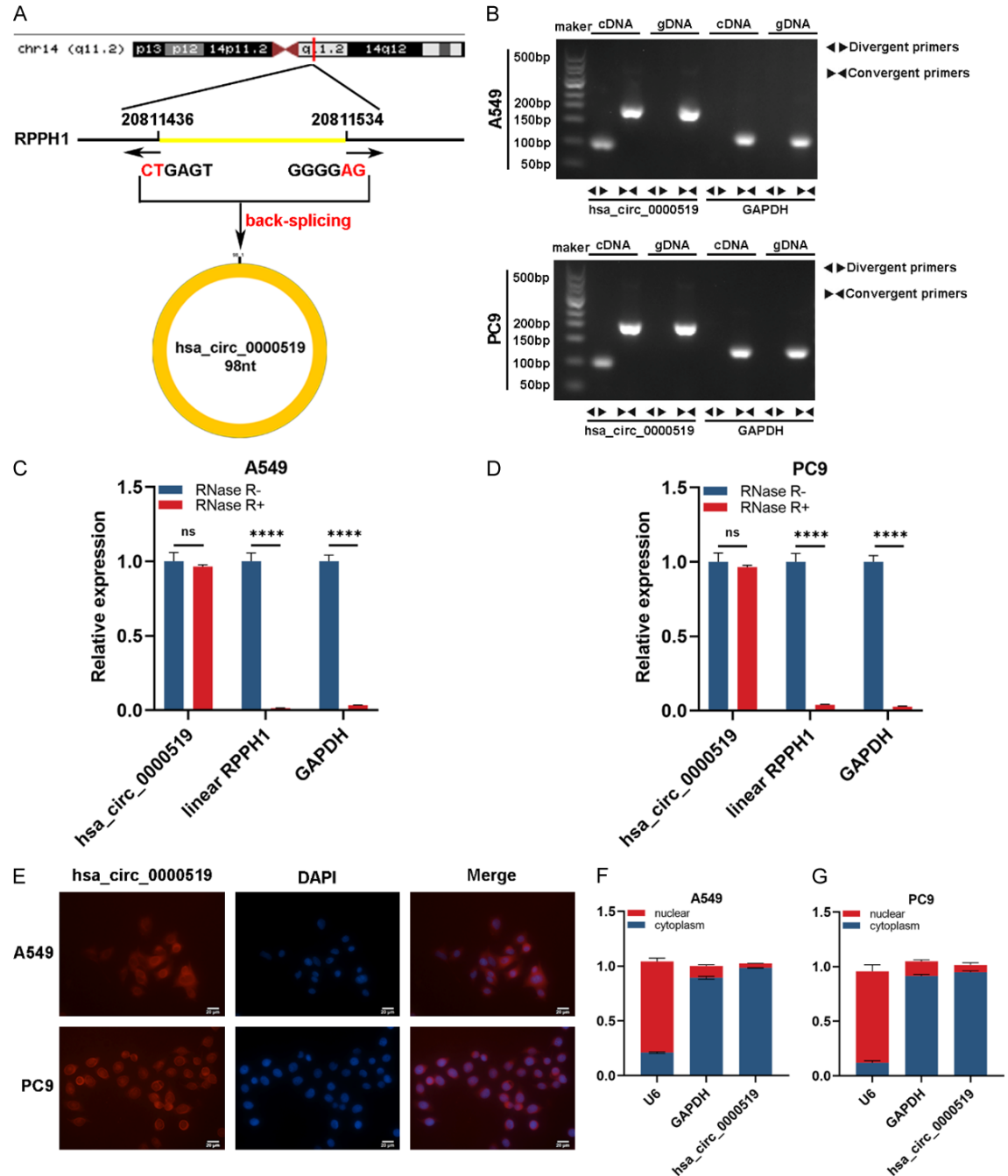
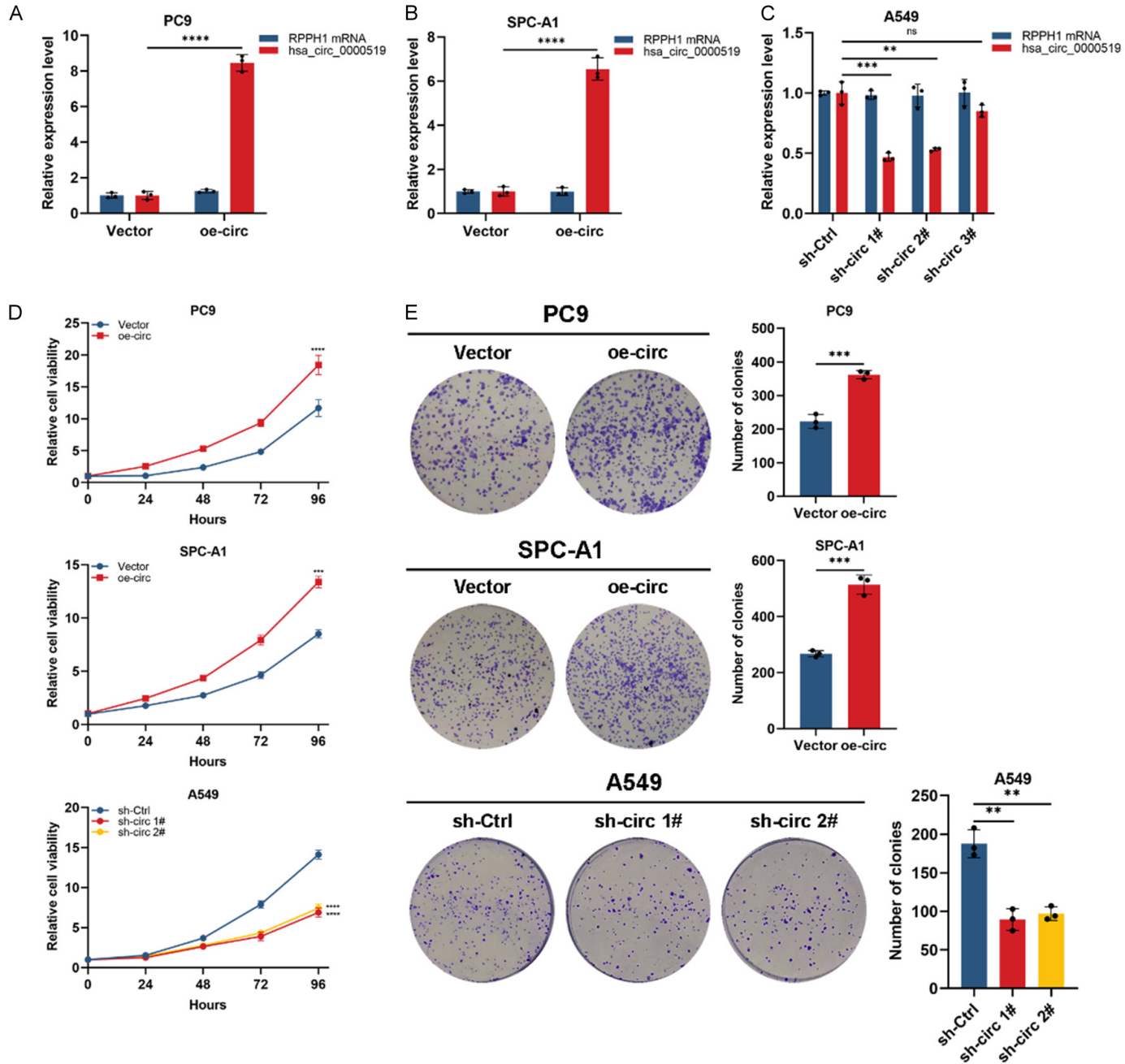


Figure 2. Characterization of hsa_circ_0000519. A. Diagrammatic illustration of the biogenesis of hsa_circ_0000519. B. Divergent and convergent primers for hsa_circ_0000519 were used for PCR and nucleic acid electrophoreses in both the A549 and PC9 cell lines. C, D. After total RNA from A549 and PC cell lines was treated with or without RNase R, relative expression of hsa_circ_0000519 and RPPH1 was detected by RT-qPCR. E. Representative images of FISH assays. F, G. RT-qPCR of isolated RNAs from the nucleus and cytoplasm of A549 and PC9 cells further confirmed the cytoplasmic localization of hsa_circ_0000519.

enhanced by the upregulation of hsa_circ_0000519 but downregulated upon hsa_circ_0000519 knockdown (Figure 4F, 4G).

Taken together, these findings suggested that hsa_circ_0000519 enhanced tumor growth in vivo.

hsa_circ_0000519 promotes lung adenocarcinoma progression



hsa_circ_0000519 promotes lung adenocarcinoma progression

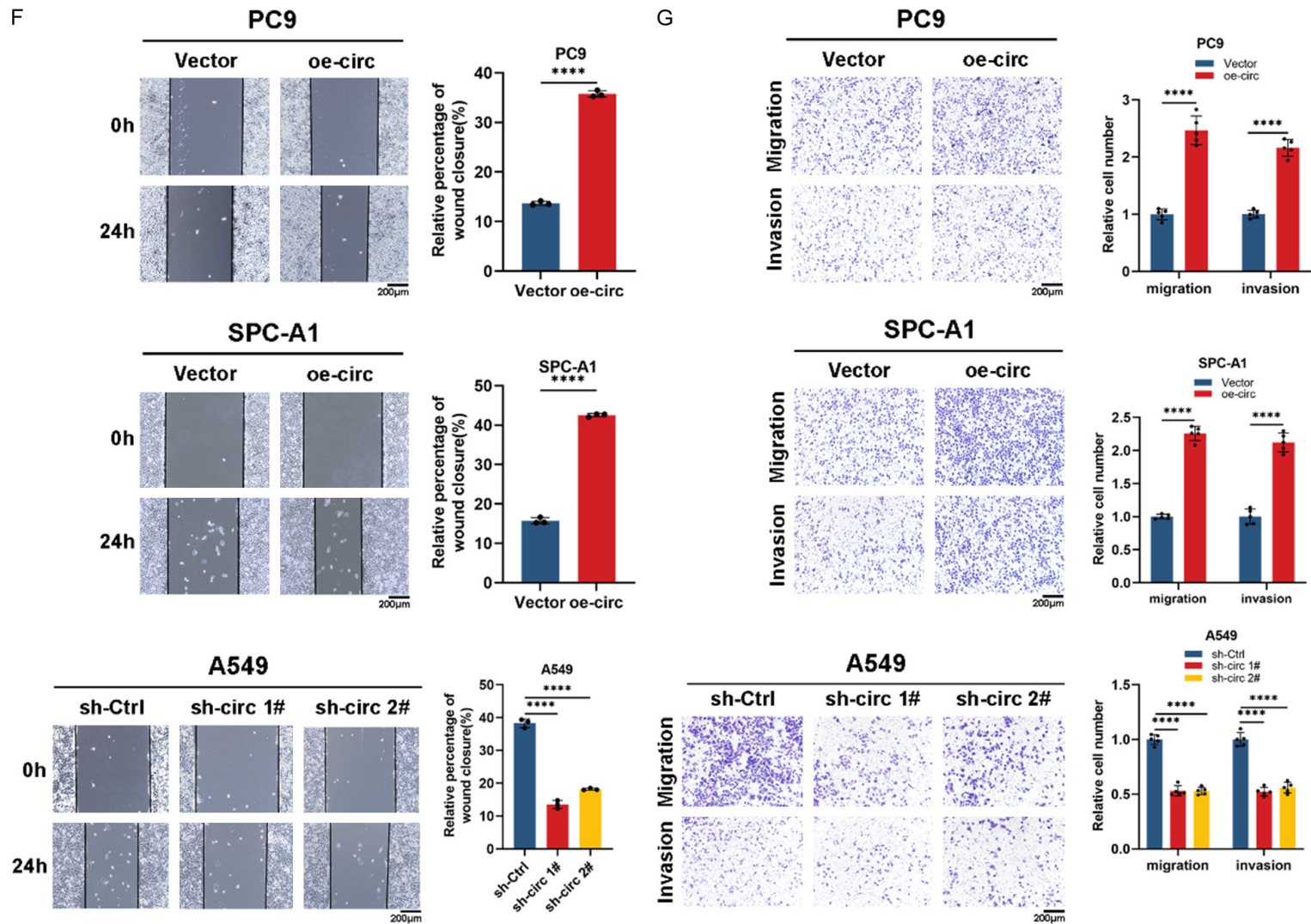


Figure 3. hsa_circ_0000519 promotes LUAD cell proliferation, migration, and invasion in vitro. A-C. Stable transfection efficiencies of hsa_circ_0000519 overexpression or knockdown in PC9, SPC-A1, and A549 cell lines. D, E. The impacts of hsa_circ_0000519 on LUAD cell proliferation were evaluated by CCK8 and colony formation assays. F, G. The effects of hsa_circ_0000519 on LUAD cell migration and invasion were investigated using wound healing and transwell assays.

hsa_circ_0000519 promotes lung adenocarcinoma progression

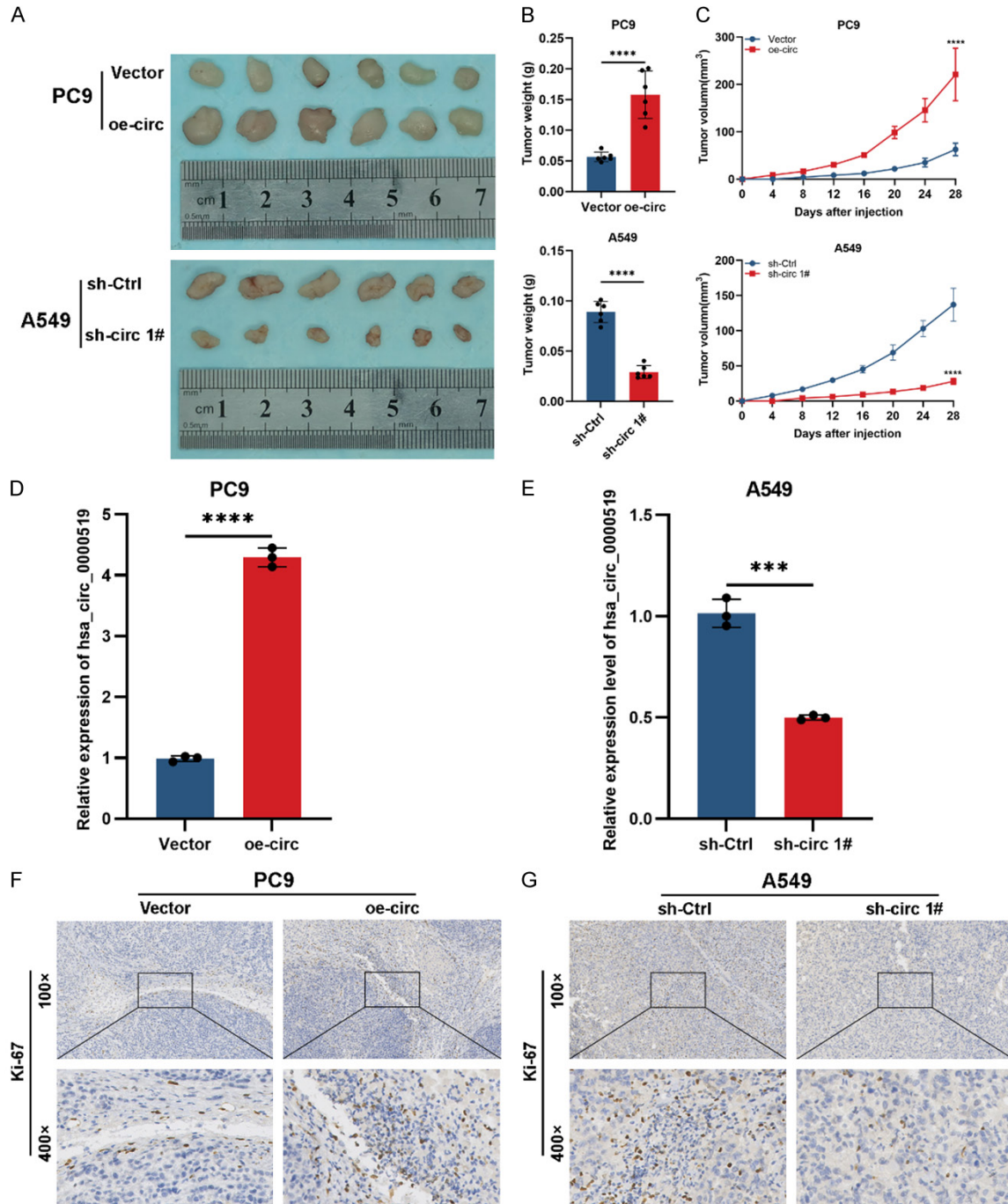


Figure 4. hsa_circ_0000519 promotes LUAD carcinogenesis in vivo. A. Images of xenograft tumor tissues in different groups. B. The weights of tumors were compared among different groups. C. Subcutaneous xenograft tumor volumes were assessed at four-day intervals. D, E. Relative hsa_circ_0000519 expression in tumor tissues was measured by RT-qPCR. F, G. IHC was used to detect Ki-67 expression in tumor tissues.

hsa_circ_0000519 directly binds to and negatively regulates the expression of hsa-miR-1296-5p in LUAD

The majority of circRNAs are located in the cytoplasm and are thought to be ceRNAs for

miRNAs. Given the cytoplasmic location of hsa_circ_0000519, we hypothesized that hsa_circ_0000519 may sponge miRNAs to perform its biological activity. Potential miRNA targets for hsa_circ_0000519 were predicted using three online databases: CircBank,

hsa_circ_0000519 promotes lung adenocarcinoma progression

CircInteractome, and ENCORI. hsa-miR-1296-5p was chosen for further study since it was predicted by all three databases (**Figure 5A** and [Supplementary Tables 6, 7, 8](#)). To preliminarily verify the results, dual luciferase reporter assays were performed in both PC9 and A549 cell lines. hsa_circ_0000519-WT/MUT plasmids (as shown in **Figure 5B**) were co-transfected into the A549 cell line with NC/hsa-miR-1296-5p mimics, and into the PC9 cell line with NC/hsa-miR-1296-5p inhibitor. As a result, co-transfection of hsa_circ_0000519-WT and hsa-miR-1296-5p mimics in the A549 cell line led to a substantial reduction in luciferase activity (**Figure 5C**), whereas co-transfection of hsa_circ_0000519-WT and hsa-miR-1296-5p inhibitor in the PC9 cell line increased the luciferase activity. These results, however, vanished when mutations were introduced into the binding sites for hsa-miR-1296-5p (**Figure 5C**). These results backed up the hypothesis that hsa_circ_0000519 directly interacted with hsa-miR-1296-5p.

It is well recognized that miRNAs suppress the expression of target genes by binding to the 3'UTR of the target gene through AGO2 and forming an RNA-induced silencing complex (RISC). To determine whether hsa_circ_0000519 binds to hsa-miR-1296-5p through AGO2, anti-AGO2 RIP assays were carried out in A549 and PC9 cell lines. The RNA transcripts that bind to the AGO2 protein were pulled down and examined by RT-qPCR. **Figure 5D** showed that both hsa_circ_0000519 and hsa-miR-1296-5p were highly enriched in the anti-AGO2 group.

The ceRNA theory proposes that circRNAs serve as molecular sponges, binding to miRNAs and regulating their expression. We further investigated how hsa_circ_0000519 affected hsa-miR-1296-5p expression in A549 and PC9 cell lines. Knocking down hsa_circ_0000519 in the A549 cell line led to a significantly increase in hsa-miR-1296-5p expression, whereas overexpressing hsa_circ_0000519 in the PC9 cell line had the reverse effect (**Figure 5E**). Further examination of 48 LUAD tissues and cell lines revealed a significant downregulation of hsa-miR-1296-5p (**Figure 5F, 5G**). Furthermore, it was also confirmed that the expression of hsa-miR-1296-5p has a negative correlation with that of hsa_

circ_0000519 in 48 LUAD tissues ($R = -0.3326$, $P = 0.0209$, **Figure 5H**). Collectively, these results demonstrated that hsa_circ_0000519 could bind to hsa-miR-1296-5p and adversely regulate its expression.

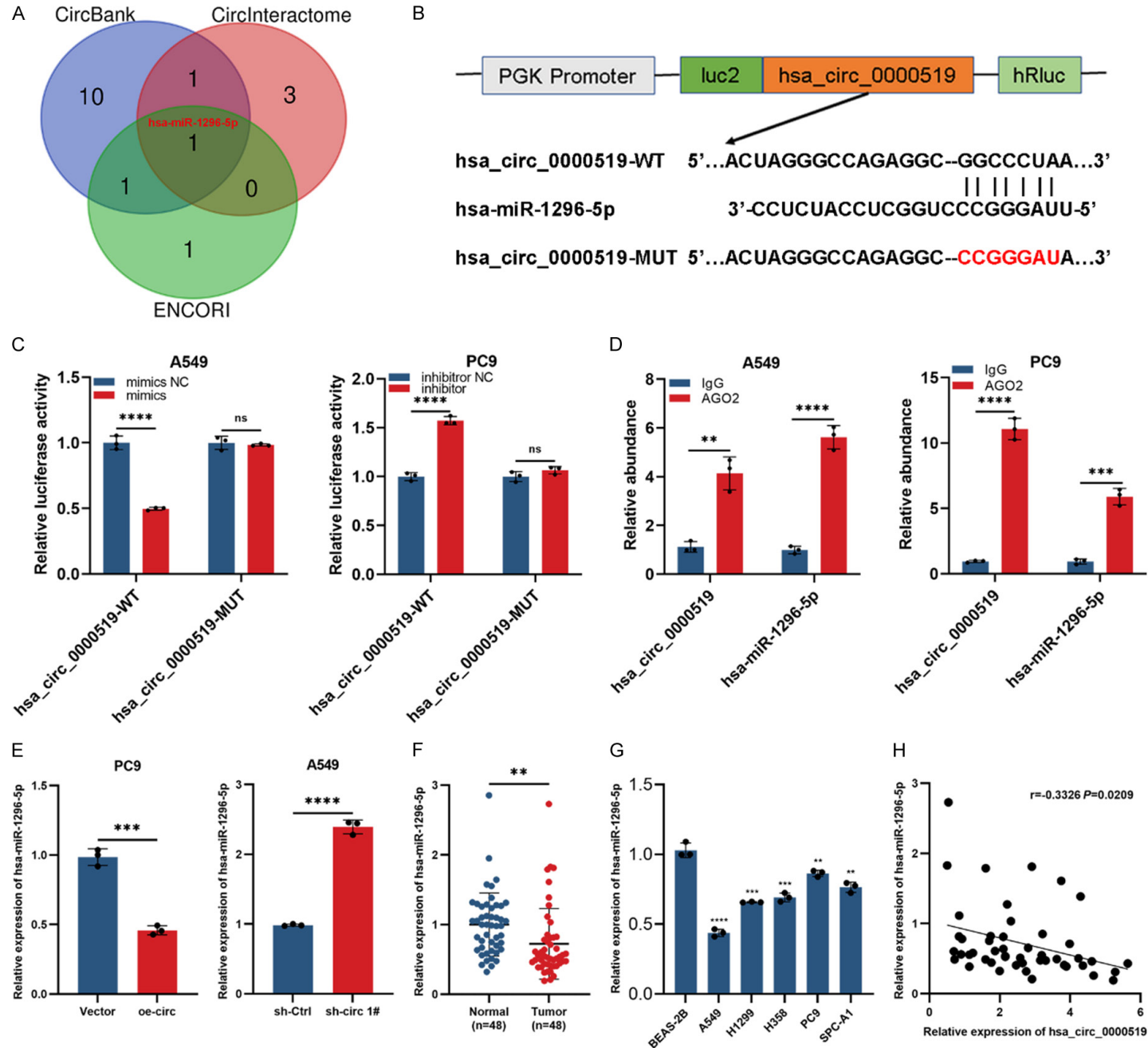
hsa-miR-1296-5p inhibits LUAD cell proliferation, migration, and invasion

Since few research have focused on hsa-miR-1296-5p's significance in LUAD, we decided to further explore its biological role. Functional studies in vitro were performed in A549 and PC9 cell lines. The transfection efficiencies were presented in [Supplementary Figure 1](#). In CCK8, we found that overexpressing hsa-miR-1296-5p greatly reduced A549 cell proliferation, but silencing its expression had the opposite effect (**Figure 6A**). Similarly, overexpression of hsa-miR-1296-5p in A549 cells decreased their capacity of colony formation, whereas inhibiting hsa-miR-1296-5p in PC9 cells improved their colony formation capacity (**Figure 6B**). Furthermore, wound healing and transwell experiments indicated that the migration and invasion of LUAD cells were considerably inhibited by the overexpression of hsa-miR-1296-5p, while downregulation of hsa-miR-1296-5p significantly enhanced these properties (**Figure 6C, 6D**). These results demonstrated that hsa-miR-1296-5p inhibited LUAD cell proliferation, migration, and invasion.

DARS is a direct target of hsa-miR-1296-5p in LUAD

After identifying hsa-miR-1296-5p as a target of hsa_circ_0000519 and its role as a tumor suppressor in LUAD, we set out to excavate its downstream target genes. Targets for hsa-miR-1296-5p were predicted by three different online databases: ENCORI, TargetScan, and Tarbase. DARS, SF3B2, and TRIP12 were retained as candidate target genes based on the overlap of prediction results (**Figure 7A** and [Supplementary Tables 9, 10, 11](#)). Then, A549 and PC9 cell lines were transfected with NC/hsa-miR-1296-5p mimics and NC/hsa-miR-1296-5p inhibitor, respectively. RT-qPCR was used to detect the difference in mRNA expression of candidate target genes. As a result, overexpressing hsa-miR-1296-5p in the A549 cell line greatly reduced DARS expression, whereas inhibition of hsa-miR-1296-5p in the

hsa_circ_0000519 promotes lung adenocarcinoma progression



hsa_circ_0000519 promotes lung adenocarcinoma progression

Figure 5. hsa_circ_0000519 has a direct interaction with hsa-miR-1296-5p. A. Bioinformatic analyses revealed that hsa-miR-1296-5p may be a direct target of hsa_circ_0000519. B. Schematic diagram to show the designation of dual luciferase plasmids. C. Dual luciferase reporter assays were performed in A549 and PC9 cells, and the luciferase activity was detected. D. Anti-AGO2 RIP tests were conducted in A549 and PC9 cells, and RT-qPCR was applied to analyze the abundance of hsa_circ_0000519 and hsa-miR-1296-5p. E. RT-qPCR was used to analyze the effect of hsa_circ_0000519 on hsa-miR-1296-5p expression. F, G. Relative expression of hsa-miR-1296-5p in 48 LUAD tissues and cell lines. H. The association of expression between hsa_circ_0000519 and hsa-miR-1296-5p expression in 48 LUAD patients.

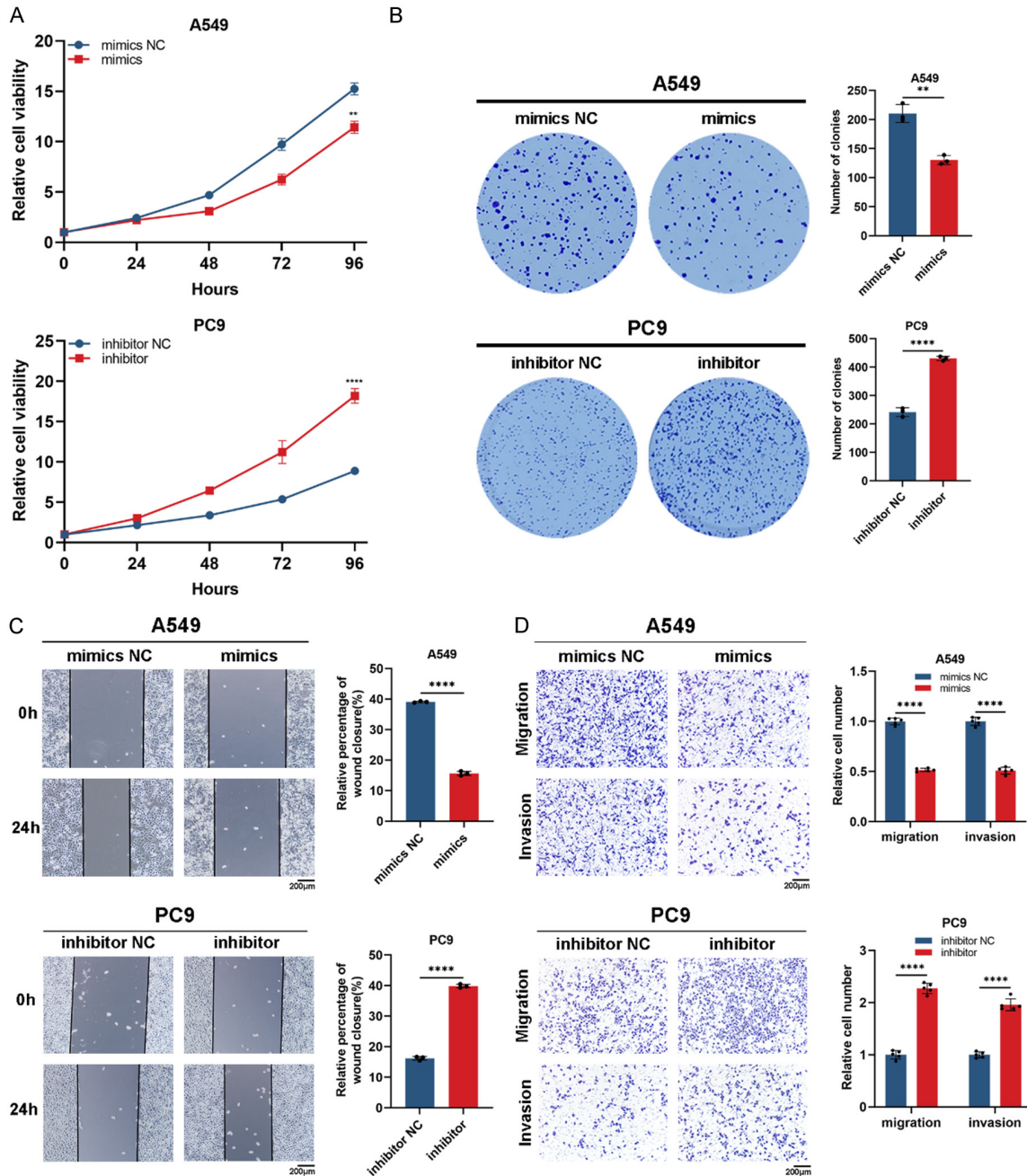
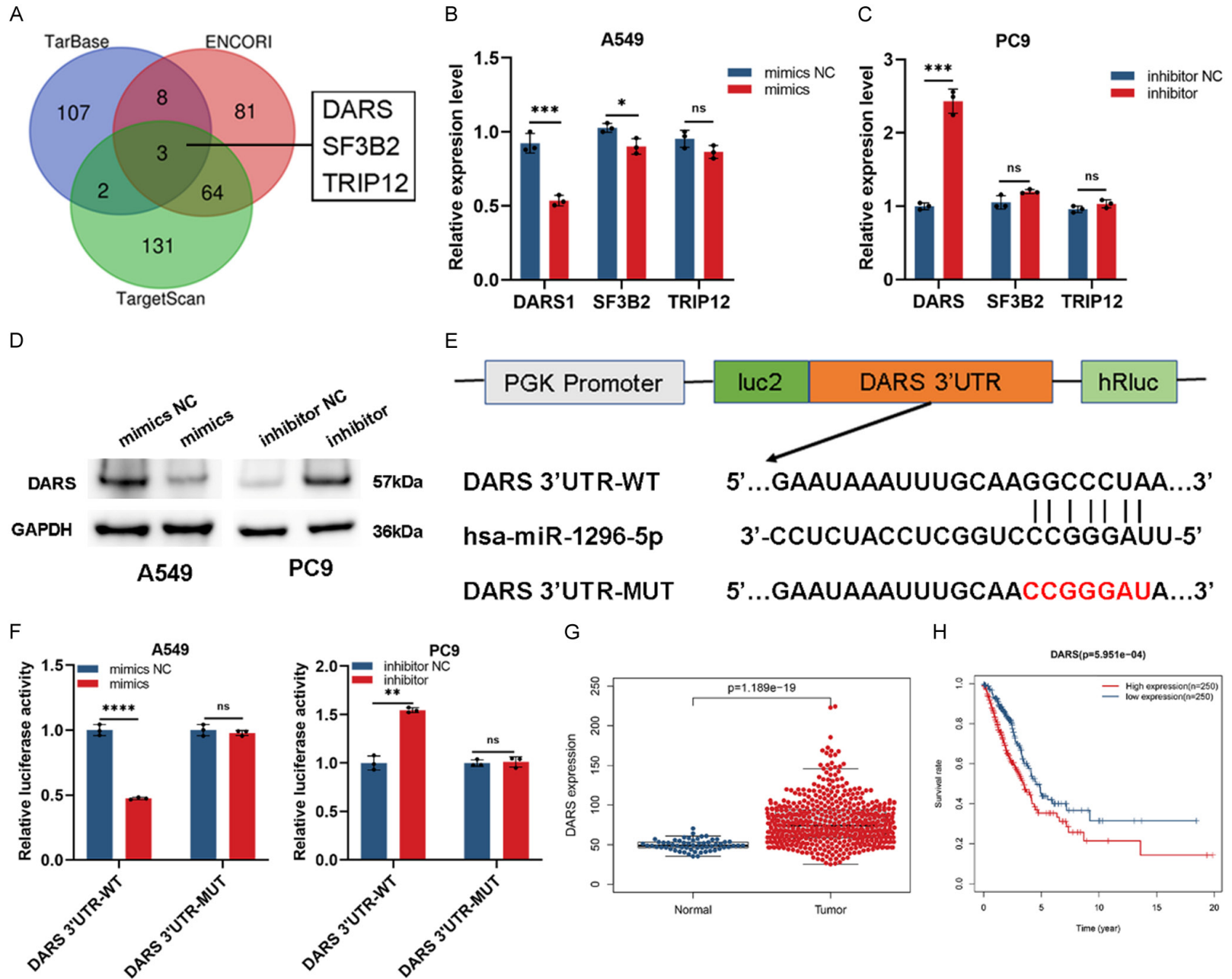


Figure 6. hsa-miR-1296-5p impeded the growth, migration, and invasion of LUAD cells. A, B. The effects of hsa-miR-1296-5p on LUAD cell proliferation were measured using CCK8 and colony formation assays. C, D. Wound healing and transwell assays were performed to analyze the impacts of hsa-miR-1296-5p on LUAD cell migration and invasion.

hsa_circ_0000519 promotes lung adenocarcinoma progression



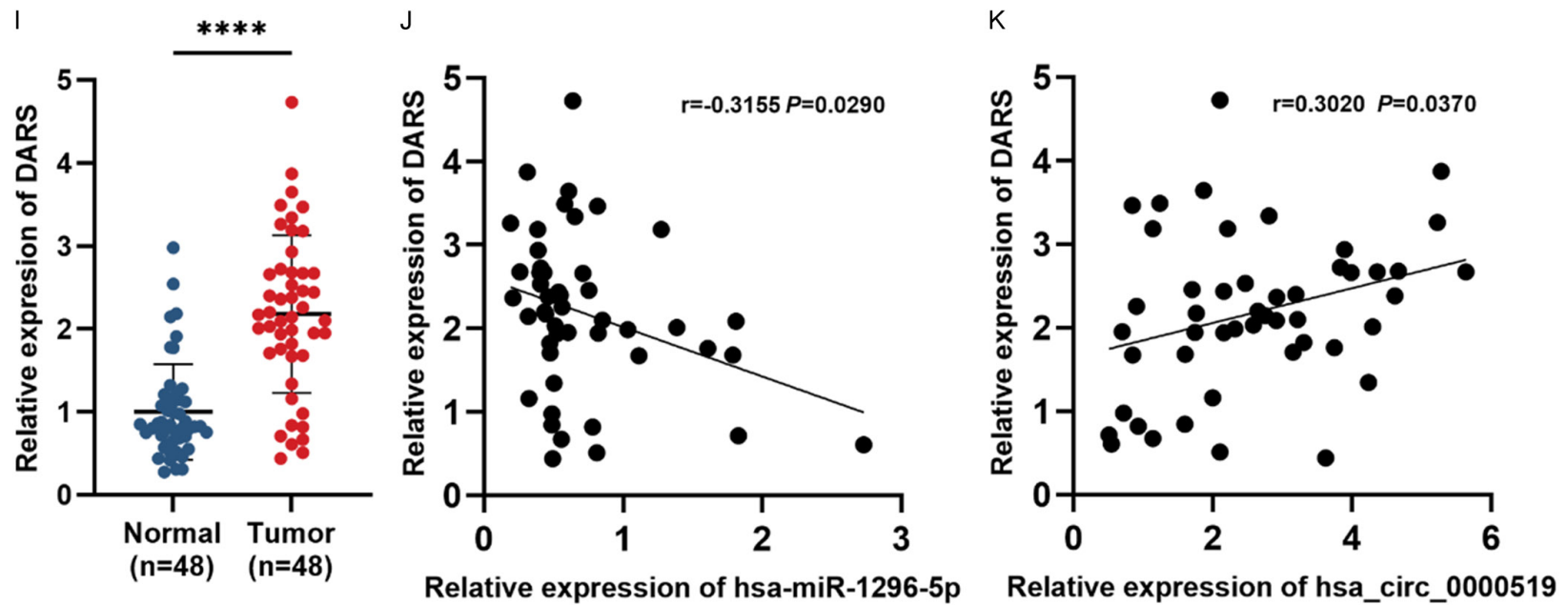


Figure 7. hsa-miR-1296-5p directly targets DARS. A. Overlap of hsa-miR-1296-5p's target genes predicted by ENCORI, TargetScan, and TarBase databases. B, C. RT-qPCR was used to analyze the impact of hsa-miR-1296-5p on candidate target genes DARS, SF3B2 and TRIP12. D. Western blotting was used to analyze the impact of hsa-miR-1296-5p on DARS protein. E. Schematic diagram to show the designation of dual luciferase plasmids. F. Dual luciferase reporter assays were performed in A549 and PC9 cells, and luciferase activities were detected. G, H. DARS expression in LUAD and its correlation with survival outcomes in LUAD patients from the TCGA database were analyzed by bioinformatics. I-K. DARS expression in 48 LUAD tissues and its association with the expression of hsa-miR-1296-5p and hsa_circ_0000519.

hsa_circ_0000519 promotes lung adenocarcinoma progression

PC9 cell line enhanced it (**Figure 7B, 7C**). Expression of SF3B2 and TRIP12 did not alter noticeably in response to hsa-miR-1296-5p overexpression or inhibition. Thus, DARS was chosen for future study. We also performed western blotting to determine the impact of hsa-miR-1296-5p on DARS protein. Similarly, DARS protein expression was suppressed by the overexpression of hsa-miR-1296-5p but enhanced by hsa-miR-1296-5p inhibition (**Figure 7D**). To our surprise, upregulation of hsa_circ_0000519 in the PC9 cell line also led to an increase in DARS mRNA and protein, while hsa_circ_0000519 knockdown exhibited the opposite effects ([Supplementary Figure 2](#)), suggesting a potential regulatory axis of hsa_circ_0000519/hsa-miR-1296-5p/DARS.

Additionally, DARS 3'UTR-WT/MUT plasmids were designed for dual luciferase reporter assays (**Figure 7E**). It was observed that co-transfection of A549 cells with hsa-miR-1296-5p mimics and DARS 3'UTR-WT dramatically decreased the luciferase activity (**Figure 7F**), whereas co-transfection of PC9 cells with hsa-miR-1296-5p inhibitor and DARS 3'UTR-WT considerably enhanced the luciferase activity. First-line evidence for the interaction between hsa-miR-1296-5p and DARS was provided by the fact that the aforementioned phenomenon vanished when the binding sites for hsa-miR-1296-5p were mutated.

Up to now, the research on DARS in LC is still blank. To confirm the expression pattern of DARS in LUAD, we first performed a bioinformatic analysis of the difference in DARS expression between 535 LUAD tissues and 59 normal lung tissues from the TCGA database. The results indicated a significant overexpression of DARS in LUAD tissues (**Figure 7G** and [Supplementary Table 12](#)). Furthermore, in Kaplan-Meier survival analysis, a higher expression level of DARS indicated a worse prognosis in patients with LUAD (**Figure 7H**). Next, RT-qPCR was utilized to verify the expression pattern of DARS in 48 LUAD samples and their matched normal lung tissues. Consistent with the results of bioinformatic analysis, DARS expression was significantly elevated in LUAD tissues (**Figure 7I**). Furthermore, Pearson analysis revealed a negative relationship between the expression of hsa-miR-1296-5p and DARS in 48 LUAD patients ($R = -0.3155$, $P = 0.029$,

Figure 7J). Notably, we also found that hsa_circ_0000519 and DARS had a positive association in expression ($R = 0.302$, $P = 0.037$, **Figure 7K**). These findings demonstrated that hsa-miR-1296-5p directly targeted DARS.

DARS could modulate the function of hsa_circ_0000519 on LUAD cell proliferation, migration, and invasion

In light of the expression association between hsa_circ_0000519 and DARS, we hypothesized that DARS may regulate hsa_circ_0000519's biological function. The PC9-vector/oe-circ were co-transfected with NC/si-DARS, and the A549-ctrl/sh-circ 1# were co-transfected with vector/oe-DARS. DARS expression was measured at the mRNA and protein levels ([Supplementary Figure 3](#)). Then, functional studies in vitro were conducted. As shown by CCK8 and colony formation assays (**Figure 8A, 8B**), overexpression of hsa_circ_0000519 considerably increased the proliferative ability of PC9 cells, whereas downregulation of DARS partly reversed this effect. In contrast, the opposite effects were observed in A549 cells. Furthermore, wound healing and transwell assays indicated that the migrative and invasive ability of PC9 cells were substantially enhanced by overexpression of hsa_circ_0000519 but were partially rescued by the downregulation of DARS, while the opposite tendencies were found in A549 cells (**Figure 8C, 8D**).

hsa_circ_0000519 promotes LUAD cell proliferation, migration, and invasion via regulating the hsa-miR-1296-5p/DARS axis and activating the PI3K/AKT/mTOR signaling pathway

To further validate whether hsa_circ_0000519 served its oncogenic role through the hsa_circ_0000519/hsa-miR-1296-5p/DARS regulatory axis, recovery experiments of molecular mechanisms were schemed by employing hsa-miR-1296-5p mimics or inhibitor. The results showed that overexpressing hsa_circ_0000519 led to an increase in DARS expression in the PC9 cell line, while co-transfection of hsa-miR-1296-5p mimics rescued this impact (**Figure 9A**). Conversely, downregulation of hsa_circ_0000519 suppressed DARS expression in the A549 cell line, while this effect was rescued by the co-transfection of hsa-miR-1296-5p inhibitor (**Figure 9B**). These findings suggested that

hsa_circ_0000519 promotes lung adenocarcinoma progression

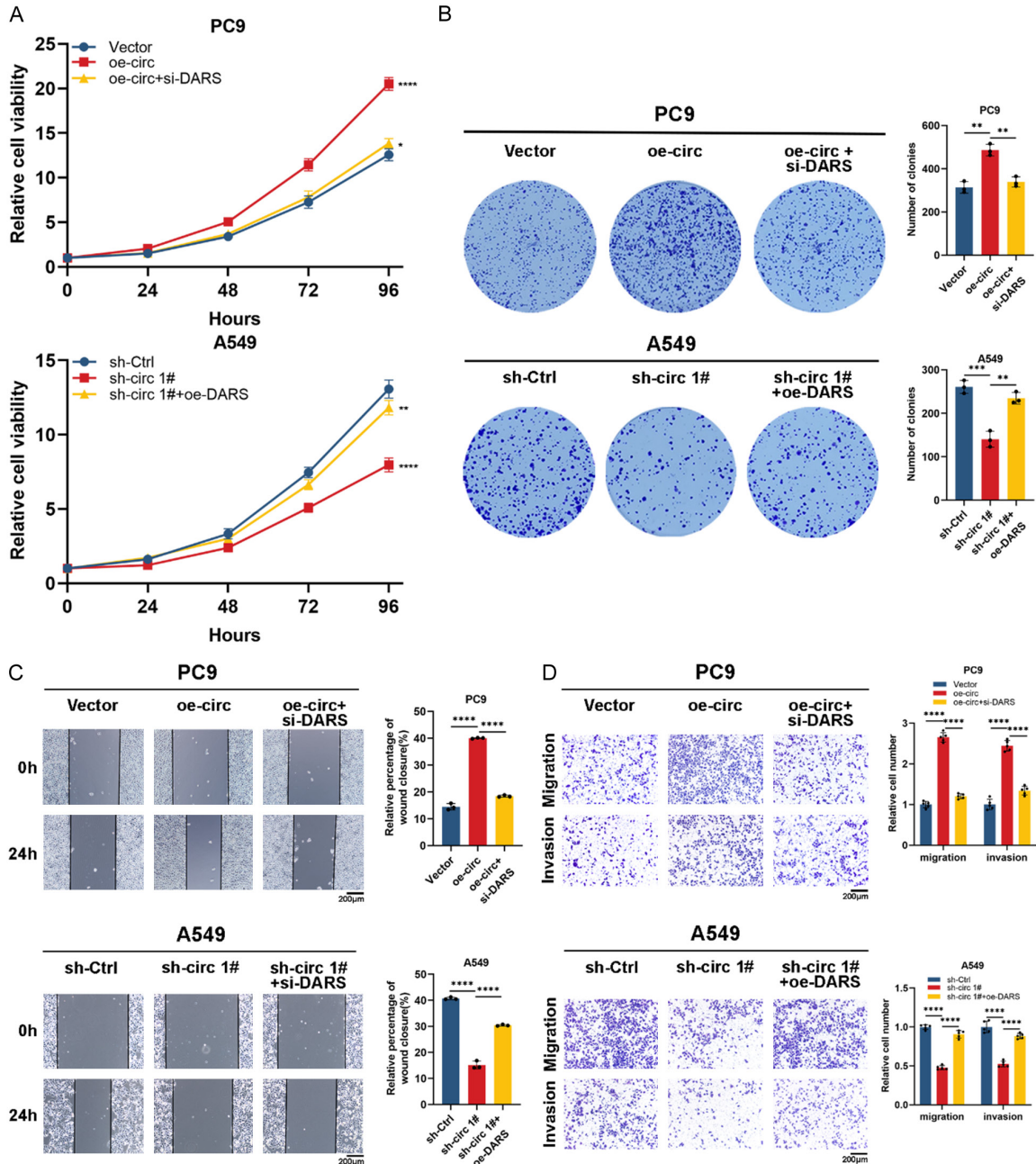


Figure 8. hsa_circ_0000519 promotes LUAD cell growth, migration, and invasion in a DARS-dependent manner. A, B. Cell proliferation was measured using CCK8 and colony formation assays in treated cells. C, D. Cell migration and invasion were analyzed using wound healing and transwell assays in treated cells.

hsa_circ_0000519 regulates DARS expression in a hsa-miR-1296-5p-dependent manner, thus forming the hsa_circ_0000519/hsa-miR-1296-5p/DARS regulatory axis. We also determined whether or not hsa-miR-1296-5p mimics/inhibitor might reverse the malignant phenotypes induced by hsa_circ_0000519. The overexpression of hsa_circ_0000519 resulted

in a proliferation enhancement in PC9 cells, which could be rescued by hsa-miR-1296-5p mimics as shown in CCK8 and colony formation assays (Figure 9C). Similar results were found in A549 cells, where hsa-miR-1296-5p inhibitor could rescue the cell proliferation suppressing effects of hsa_circ_0000519 knockdown (Figure 9D). Furthermore, the hsa-miR-1296-

hsa_circ_0000519 promotes lung adenocarcinoma progression

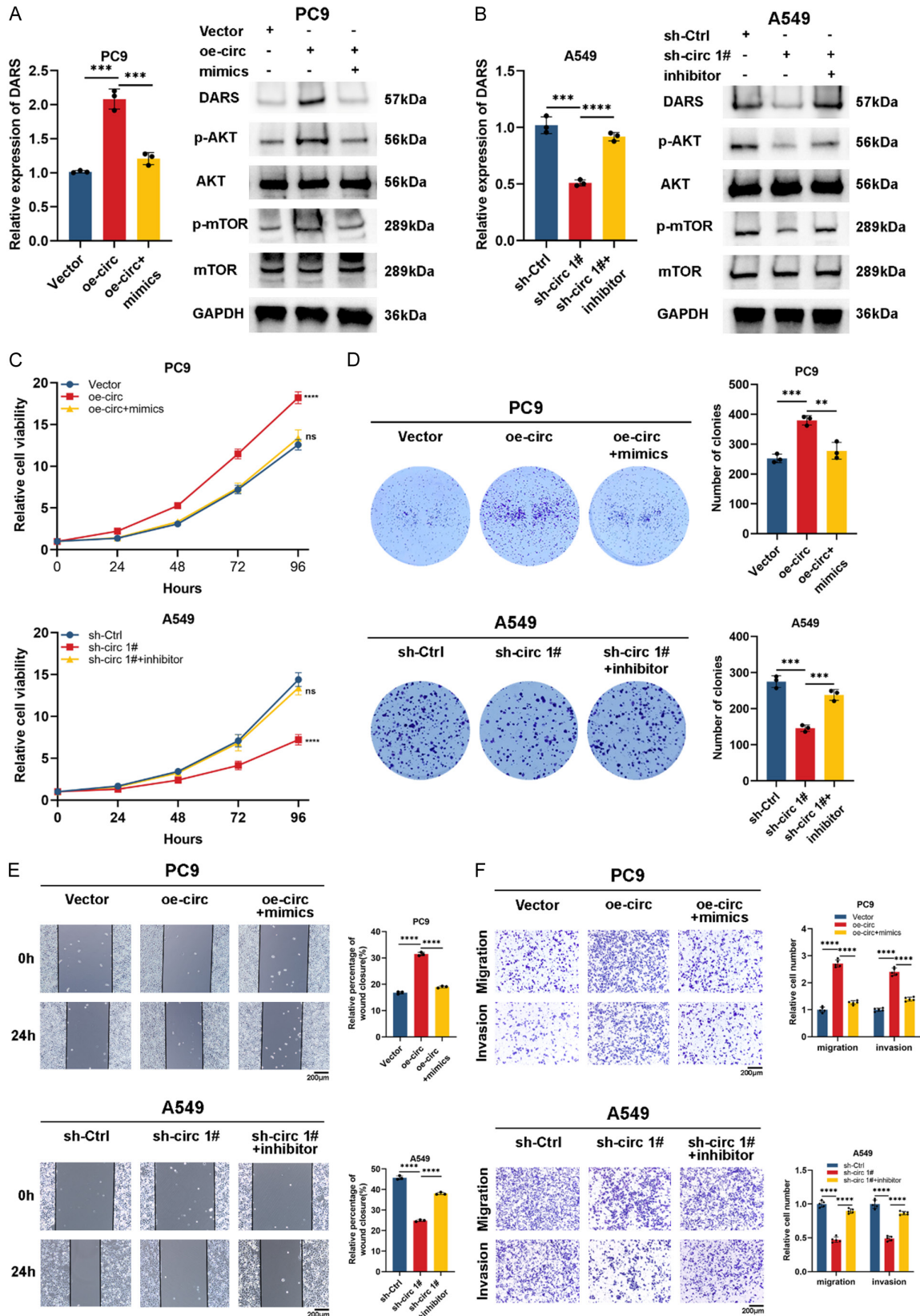


Figure 9. hsa_circ_0000519 accelerates LUAD cell proliferation, migration, and invasion through the hsa-miR-1296-5p/DARS axis. A, B. Following transfection of PC9 and A549 cell lines with the specified oe-circ, sh-circ 1#, hsa-miR-1296-5p mimics, or inhibitor, RT-qPCR and western blotting were utilized to measure the mRNA and protein

hsa_circ_0000519 promotes lung adenocarcinoma progression

expression levels, respectively. C, D. Cell proliferation was evaluated using CCK8 and colony formation assays in treated cells. E, F. Wound healing and transwell assays were performed to determine the migration and invasion of the treated cells.

Table 2. Gene set enrichment analysis (GSEA) substantially enriched pathways in high and low DARS expression groups

Enriched pathways	SIZE	ES	NES	NOM p-val	FDR q-val
DARS high expression group					
MTORC1_SIGNALING	197	0.77	2.47	0.000	0.000
MYC_TARGETS_V1	195	0.89	2.47	0.000	0.000
G2M_CHECKPOINT	196	0.84	2.44	0.000	0.000
GLYCOLYSIS	198	0.66	2.4	0.000	0.000
PI3K_AKT_MTOR_SIGNALING	110	0.68	2.4	0.000	0.000
E2F_TARGETS	198	0.89	2.38	0.000	0.000
PROTEIN_SECRETION	96	0.63	2.22	0.002	0.000
DNA_REPAIR	149	0.65	2.17	0.000	0.001
MYC_TARGETS_V2	57	0.84	2.14	0.000	0.001
SPERMATOGENESIS	133	0.53	2.02	0.000	0.004
OXIDATIVE_PHOSPHORYLATION	200	0.7	1.95	0.002	0.007
HYPOXIA	197	0.51	1.91	0.002	0.011
MITOTIC_SPINDLE	198	0.54	1.89	0.006	0.012
UNFOLDED_PROTEIN_RESPONSE	105	0.45	1.81	0.012	0.019
FATTY_ACID_METABOLISM	156	0.49	1.75	0.016	0.026
UV_RESPONSE_UP	156	0.44	1.7	0.004	0.035
ADIPOGENESIS	198	0.44	1.68	0.008	0.037
ANDROGEN_RESPONSE	99	0.41	1.61	0.033	0.055
PEROXISOME	104	0.4	1.52	0.022	0.083
DARS low expression group					
MYOGENESIS	199	-0.49	-1.87	0.004	0.114
P53_PATHWAY	196	-0.38	-1.51	0.046	0.236
KRAS_SIGNALING_DN	199	-0.38	-1.61	0.008	0.238

5p mimics reversed the promoting effects of hsa_circ_0000519 on the migrative and invasive abilities of PC9 cells, and similar results were observed in A549 cells transfected with sh-circ 1# and hsa-miR-1296-5p inhibitor (**Figure 9E, 9F**). These findings as a whole suggested that hsa_circ_0000519 promoted the progression of LUAD by serving as a miRNA sponge for hsa-miR-1296-5p to upregulate DARS expression.

Disturbances in signaling pathways that regulate normal cell growth, differentiation, proliferation, and apoptosis are a common feature of malignant neoplasms [40, 41]. We further explored potential signaling pathways involved in the hsa_circ_0000519/hsa-miR-1296-5p/DARS axis. First, GSEA was used to screen pos-

sible signaling pathways affected by DARS dysregulation. As a result, 22 distinct signaling pathways were identified (**Table 2**). The results indicated that most of the significantly enriched signaling pathways in the DARS high expression group were closely associated with tumorigenesis and cancer progression (**Supplementary Figure 4**). Considering the central role of the PI3K/AKT/mTOR signaling pathway in controlling cancer cell proliferation, migration, and invasion, we further investigated whether the PI3K/AKT/mTOR signaling pathway had any association with the hsa_circ_0000519/hsa-miR-1296-5p/DARS axis. The results showed that the upregulation of hsa_circ_0000519 in the PC9 cell line increased p-AKT and p-mTOR expression, but had no effect on total AKT and mTOR levels. Meanwhile, co-transfection of

hsa-miR-1296-5p mimics in the PC9 cell line partially rescued the positive effects of hsa_circ_0000519 on p-AKT and p-mTOR expression (**Figure 9A**). The results in the A549 cell line were contrary to those seen in the PC9 cell line (**Figure 9B**). These data indicated that hsa_circ_0000519 activated the PI3K/AKT/mTOR signaling pathway by modulating the hsa-miR-1296-5p/DARS axis.

Discussion

LUAD is the most frequent pathologic subtype of NSCLC, accounting for about half of all LC cases. Unfortunately, the prognosis for LUAD patients hasn't improved much despite advances in diagnosis and therapy [42]. Therefore, novel LUAD biomarkers and treatment targets are desperately needed. Recent research has shown that circRNAs are essential in many biological processes, and their dysregulation is linked to cancer development and progression [10, 43]. In the present study, we revealed a LUAD-associated circRNA hsa_circ_0000519 acting as a ceRNA for hsa-miR-1296-5p to promote the progression of LUAD.

Bioinformatic analyses of three circRNA microarray datasets from the GEO database first revealed the LUAD-related circRNA hsa_circ_0000519, and the high expression of hsa_circ_0000519 was identified in LUAD tissues and cell lines, which was corroborated with a recent publication by Wang et al. [44]. In the current study, we also found a positive correlation between the expression of hsa_circ_0000519 and T grade as well as TNM stage of LUAD patients. Second, we performed a series of functional experiments in both vitro and vivo to demonstrate that hsa_circ_0000519 accelerates LUAD cell proliferation, migration, and invasion. Third, as a target of hsa_circ_0000519, hsa-miR-1296-5p was identified to be significant downregulation in LUAD tissues and inversely linked with the proliferation, migration, and invasion of LUAD cells. Fourth, mechanism exploration demonstrated that hsa_circ_0000519 acted as a miRNA sponge for hsa-miR-1296-5p to upregulate DARS expression and activate the PI3K/AKT/mTOR signaling pathway. Collectively, our results implied that hsa_circ_0000519 is critically involved in LUAD progression.

The subcellular localization of circRNAs has largely determined their function. We confirmed the cytoplasmic localization of hsa_circ_0000519, where circRNAs bind RBP, encode peptides, or act as miRNA sponges [45]. Since the vast majority of circRNAs are exported to the cytoplasm and contain miRNA response elements (MREs), which allow for the interaction with miRNA, the miRNA sponge is considered to be the most prevalent and essential function of circRNAs [46, 47]. By competitively sponging miR-326 to upregulate FSCN1 [48], for instance, circSATB2 promoted NSCLC cell proliferation, migration, and invasion. The upregulation of circFOXM1 had been linked to its ability to increase FAM83D expression, through which circFOXM1 increased NSCLC cell proliferation in both vitro and vivo. Meanwhile, miR-614 was able to repress FAM83D expression and restrain NSCLC cell proliferation, while circFOXM1 facilitated this process by binding to miR-614 and overriding its repression of FAM83D expression [49]. Consistent with an earlier investigation by Yi Liu et al. [50], our study demonstrated the direct interaction between hsa_circ_0000519 and hsa-miR-1296-5p by RIP and dual luciferase reporter assays. Furthermore, recovery experiments showed that hsa-miR-1296-5p counteracted the malignant phenotype-promoting effects of hsa_circ_0000519. Consequently, our findings demonstrated that hsa_circ_0000519 acted as a sponge for hsa-miR-1296-5p.

Protein translation is performed by the ribosome, which uses amino-acylated tRNA to decode mRNA transcripts, while aminoacyl-tRNA synthetases (ARSs) complete the amino-acylation of tRNA by ligating amino acids to their homologous tRNA, hence ARSs are essential for protein translation [51]. As a member of the ARSs superfamily, DARS primarily mediates the binding of aspartic acid to homologous tRNAs [24]. Prior to this study, the role of DARS in carcinogenesis and progression was little known. Next-generation sequencing (NGS), bioinformatics analysis of the TCGA database, and immunohistochemistry were implemented by Bin Liu et al. to uncover the high expression of DARS in gastric cancer, where they discovered that a high level of DARS protein expression correlated with more advanced TNM stag-

es and a poorer prognosis for patients with gastric cancer. Meanwhile, knockdown of DARS expression significantly inhibited the proliferative ability of gastric cancer cells [22]. In addition, DARS-AS1, an elevated lncRNA in clear cell renal carcinoma, was shown to increase cellular proliferation ability by competitively absorbing miR-194-5p and increasing DARS expression. Further investigations revealed that clear cell renal carcinoma tissues showed a high level of DARS expression and that a decrease in DARS expression resulted in the suppression of cell growth, suggesting an oncogenic function for DARS in clear cell renal carcinoma [26]. However, the research on the expression and biological role of DARS in LC is still blank. Our present study revealed the elevation of DARS expression in LUAD tissues, which was correlated with a dismal prognosis for LUAD patients. In addition, the pro-oncogenic role of DARS in LUAD was supported by the fact that hsa_circ_0000519 promoted the proliferation, migration, and invasion of LUAD cells in a DARS-dependent manner. However, further research was required to fully comprehend both the functional role and mechanism of DARS in LUAD progression.

By abnormally modulating fundamental cellular functions, such as cell proliferation, migration, apoptosis, and angiogenesis, et al. [52, 53], the PI3K/AKT/mTOR signaling pathway is essential for cancer initiation and development. Recent research has shown that circRNAs may regulate tumor progression by interacting with the PI3K/AKT/mTOR signaling pathway. Taoyue Yang et al. [54], for instance, reported that FUS-mediated circRHOBTB3 could activate the AKT/mTOR signaling pathway by acting as a miR-600 sponge to sustain NACC1 expression, therefore suppressing autophagy and promoting the development of pancreatic ductal cancer. Furthermore, hsa_circ_0001666 was overexpressed in NSCLC tissues and cell lines, and was linked to a worse prognosis in LUAD patients. Knocking down hsa_circ_0001666 has the functional effect of slowing NSCLC cell proliferation, migration, and invasion. Mechanically, hsa_circ_0001666 competitively sponged miR-1184 to upregulate AGO1, which in turn activated the PI3K/AKT/mTOR signaling pathway [55]. In this study, we found that DARS dysregulation is potentially

involved in the control of the PI3K/AKT/mTOR signaling pathway by GSEA. Then, the regulatory effects of the hsa_circ_0000519/hsa-miR-1296-5p/DARS axis on the PI3K/AKT/mTOR signaling pathway were confirmed by recovery experiments. Collectively, our findings suggested that hsa_circ_0000519 could promote the progression of LUAD by competitively sponging hsa-miR-1296-5p to regulate DARS expression and activate the PI3K/AKT/mTOR signaling pathway.

To our knowledge, this is the first research to demonstrate the interactions between hsa_circ_0000519, hsa-miR-1296-5p, and DARS. In addition, we first determined the expression pattern and biological role of DARS in LUAD. These findings may shed light on the therapy for LUAD. Though our study still has some limitations. First, our data gathered in vitro and in vivo indicated that hsa_circ_0000519 functions as an oncogene to promote LUAD progression. More research on hsa_circ_0000519 expression in bodily fluids is needed to determine its potential as an optimal tumor biomarker and viable treatment target for LUAD. Second, the detailed mechanism by which DARS influences the malignant phenotypes of LUAD cells has yet to be understood, despite the fact that it was first discovered to be significantly upregulated in LUAD tissues. Third, further research is needed to determine whether cytoplasmic hsa_circ_0000519 may influence LUAD progression via other mechanisms, such as through interactions with RNA-binding proteins. Therefore, further research is needed to fully appreciate hsa_circ_0000519's role in LUAD.

Conclusions

hsa_circ_0000519 is significantly upregulated in LUAD tissues and cell lines. By competitively sponging hsa-miR-1296-5p and reducing its repressive impact on DARS, hsa_circ_0000519 promotes the progression of LUAD (as shown in **Figure 10**). hsa_circ_0000519 may be expected as a novel biomarker and therapeutic for LUAD.

Acknowledgements

This research was funded by the National Natural Science Foundation of China (8197-

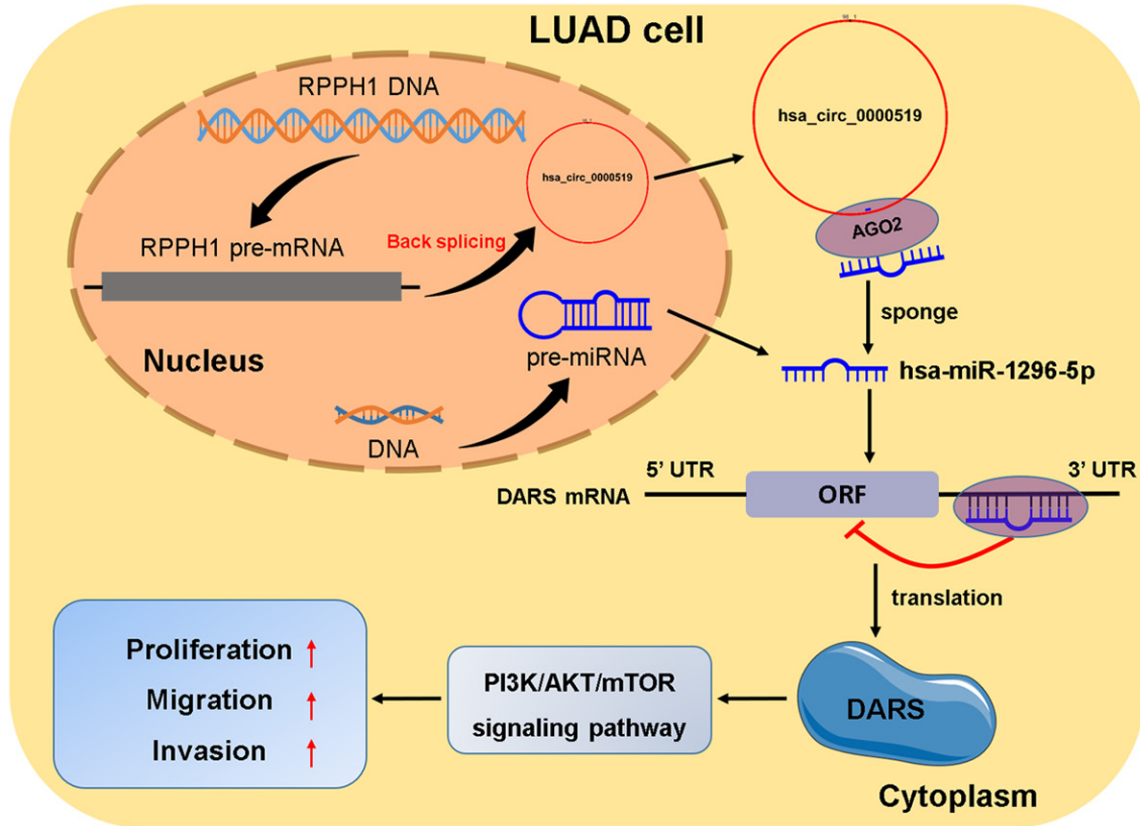


Figure 10. This study demonstrates that hsa_circ_0000519 promotes the progression of lung adenocarcinoma. hsa_circ_0000519 could regulate the expression of DARS by competitively sponging hsa-miR-1296-5p. hsa_circ_0000519 activates the PI3K/AKT/mTOR signaling pathway.

2195; 82172879), Hunan Provincial Key Area R&D Programmes (2020SK53424), and the Natural Science Foundation of Hunan Province (2021JJ30957).

Disclosure of conflict of interest

None.

Address correspondence to: Xiang Wang, Department of Thoracic Surgery, The Second Xiangya Hospital, Central South University, Changsha 410011, Hunan, China. E-mail: wangxiang@csu.edu.cn

References

[1] Sung H, Ferlay J, Siegel RL, Laversanne M, Soerjomataram I, Jemal A and Bray F. Global cancer statistics 2020: GLOBOCAN estimates of incidence and mortality worldwide for 36 cancers in 185 countries. *CA Cancer J Clin* 2021; 71: 209-249.

- [2] Siegel RL, Miller KD, Wagle NS and Jemal A. Cancer statistics, 2023. *CA Cancer J Clin* 2023; 73: 17-48.
- [3] Zheng R, Zhang S, Zeng H, Wang S, Sun K, Chen R, Li L, Wei W and He J. Cancer incidence and mortality in China, 2016. *J Natl Cancer Cent* 2022; 2: 1-9.
- [4] Herbst RS, Morgensztern D and Boshoff C. The biology and management of non-small cell lung cancer. *Nature* 2018; 553: 446-454.
- [5] Zhang LX, Gao J, Long X, Zhang PF, Yang X, Zhu SQ, Pei X, Qiu BQ, Chen SW, Lu F, Lin K, Xu JJ and Wu YB. The circular RNA circHMGB2 drives immunosuppression and anti-PD-1 resistance in lung adenocarcinomas and squamous cell carcinomas via the miR-181a-5p/CARM1 axis. *Mol Cancer* 2022; 21: 110.
- [6] Denisenko TV, Budkevich IN and Zhivotovskiy B. Cell death-based treatment of lung adenocarcinoma. *Cell Death Dis* 2018; 9: 117.
- [7] Macheleidt IF, Dalvi PS, Lim SY, Meemboor S, Meder L, Käsgen O, Müller M, Kleemann K, Wang L, Nürnberg P, Rüsseler V, Schäfer SC, Mahabir E, Büttner R and Odenthal M. Preclinical studies reveal that LSD1 inhibition results

hsa_circ_0000519 promotes lung adenocarcinoma progression

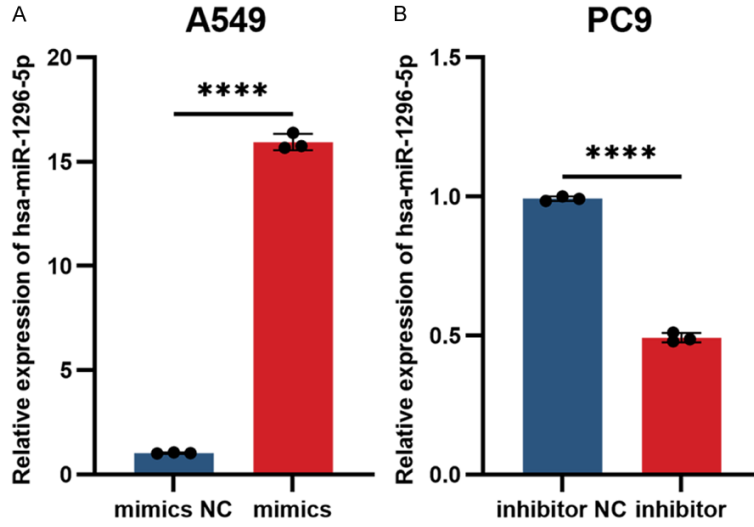
- in tumor growth arrest in lung adenocarcinoma independently of driver mutations. *Mol Oncol* 2018; 12: 1965-1979.
- [8] Kapranov P, Cheng J, Dike S, Nix DA, Duttagupta R, Willingham AT, Stadler PF, Hertel J, Hackermüller J, Hofacker IL, Bell I, Cheung E, Drenkow J, Dumais E, Patel S, Helt G, Ganesh M, Ghosh S, Piccolboni A, Sementchenko V, Tammana H and Gingeras TR. RNA maps reveal new RNA classes and a possible function for pervasive transcription. *Science* 2007; 316: 1484-1488.
- [9] Wilusz JE and Sharp PA. Molecular biology. A circuitous route to noncoding RNA. *Science* 2013; 340: 440-441.
- [10] Hansen TB, Jensen TI, Clausen BH, Bramsen JB, Finsen B, Damgaard CK and Kjems J. Natural RNA circles function as efficient microRNA sponges. *Nature* 2013; 495: 384-388.
- [11] Kristensen LS, Andersen MS, Stagsted LW, Ebbesen KK, Hansen TB and Kjems J. The biogenesis, biology and characterization of circular RNAs. *Nat Rev Genet* 2019; 20: 675-691.
- [12] Kristensen LS, Jakobsen T, Hager H and Kjems J. The emerging roles of circRNAs in cancer and oncology. *Nat Rev Clin Oncol* 2022; 19: 188-206.
- [13] Li J, Sun D, Pu W, Wang J and Peng Y. Circular RNAs in cancer: biogenesis, function, and clinical significance. *Trends Cancer* 2020; 6: 319-336.
- [14] Zhang N, Nan A, Chen L, Li X, Jia Y, Qiu M, Dai X, Zhou H, Zhu J, Zhang H and Jiang Y. Circular RNA circSATB2 promotes progression of non-small cell lung cancer cells. *Mol Cancer* 2020; 19: 101.
- [15] Lei J, Zhu J, Hui B, Jia C, Yan X, Jiang T and Wang X. Circ-HSP90A expedites cell growth, stemness, and immune evasion in non-small cell lung cancer by regulating STAT3 signaling and PD-1/PD-L1 checkpoint. *Cancer Immunol Immunother* 2023; 72: 101-124.
- [16] Ashrafizadeh M, Zarrabi A, Hushmandi K, Hashemi F, Moghadam ER, Owrang M, Hashemi F, Makvandi P, Goharrizi MASB, Najafi M and Khan H. Lung cancer cells and their sensitivity/resistance to cisplatin chemotherapy: role of microRNAs and upstream mediators. *Cell Signal* 2021; 78: 109871.
- [17] Mirzaei S, Zarrabi A, Hashemi F, Zabolian A, Saleki H, Ranjbar A, Seyed Saleh SH, Bagheri-an M, Sharifzadeh SO, Hushmandi K, Liskova A, Kubatka P, Makvandi P, Tergaonkar V, Kumar AP, Ashrafizadeh M and Sethi G. Regulation of Nuclear Factor-KappaB (NF- κ B) signaling pathway by non-coding RNAs in cancer: inhibiting or promoting carcinogenesis? *Cancer Lett* 2021; 509: 63-80.
- [18] Paskeh MDA, Mirzaei S, Orouei S, Zabolian A, Saleki H, Azami N, Hushmandi K, Baradaran B, Hashmi M, Aref AR, Ertas YN, Zarrabi A, Ashrafizadeh M and Samarghandian S. Revealing the role of miRNA-489 as a new onco-suppressor factor in different cancers based on pre-clinical and clinical evidence. *Int J Biol Macromol* 2021; 191: 727-737.
- [19] Chen X, Mao R, Su W, Yang X, Geng Q, Guo C, Wang Z, Wang J, Kresty LA, Beer DG, Chang AC and Chen G. Circular RNA circHIPK3 modulates autophagy via MIR124-3p-STAT3-PRKAA/AMPK α signaling in STK11 mutant lung cancer. *Autophagy* 2020; 16: 659-671.
- [20] Pan G, Liu Y, Shang L, Zhou F and Yang S. EMT-associated microRNAs and their roles in cancer stemness and drug resistance. *Cancer Commun (Lond)* 2021; 41: 199-217.
- [21] Iqbal MA, Arora S, Prakasam G, Calin GA and Syed MA. MicroRNA in lung cancer: role, mechanisms, pathways and therapeutic relevance. *Mol Aspects Med* 2019; 70: 3-20.
- [22] Chi Y, Zheng W, Bao G, Wu L, He X, Gan R, Shen Y, Yin X and Jin M. Circular RNA circ_103820 suppresses lung cancer tumorigenesis by sponging miR-200b-3p to release LATS2 and SOCS6. *Cell Death Dis* 2021; 12: 185.
- [23] Wang ZH, Ye LL, Xiang X, Wei XS, Niu YR, Peng WB, Zhang SY, Zhang P, Xue QQ, Wang HL, Du YH, Liu Y, Ai JQ and Zhou Q. Circular RNA circFBXO7 attenuates non-small cell lung cancer tumorigenesis by sponging miR-296-3p to facilitate KLF15-mediated transcriptional activation of CDKN1A. *Transl Oncol* 2023; 30: 101635.
- [24] Klugmann M, Kalotay E, Delerue F, Ittner LM, Bongers A, Yu J, Morris MJ, Housley GD and Fröhlich D. Developmental delay and late onset HBSL pathology in hypomorphic Dars1 (M256L) mice. *Neurochem Res* 2022; 47: 1972-1984.
- [25] Liu B, Katoh H, Komura D, Yamamoto A, Ochi M, Onoyama T, Abe H, Ushiku T, Seto Y, Suo J and Ishikawa S. Functional genomics screening identifies aspartyl-tRNA synthetase as a novel prognostic marker and a therapeutic target for gastric cancers. *J Pathol* 2022; 258: 106-120.
- [26] Jiao M, Guo H, Chen Y, Li L and Zhang L. DARS-AS1 promotes clear cell renal cell carcinoma by sequestering miR-194-5p to up-regulate DARS. *Biomed Pharmacother* 2020; 128: 110323.
- [27] Liu P, Cheng H, Roberts TM and Zhao JJ. Targeting the phosphoinositide 3-kinase pathway in cancer. *Nat Rev Drug Discov* 2009; 8: 627-644.
- [28] Chen J, Alduais Y, Zhang K, Zhu X and Chen B. CCAT1/FABP5 promotes tumour progression through mediating fatty acid metabolism and stabilizing PI3K/AKT/mTOR signalling in lung

hsa_circ_0000519 promotes lung adenocarcinoma progression

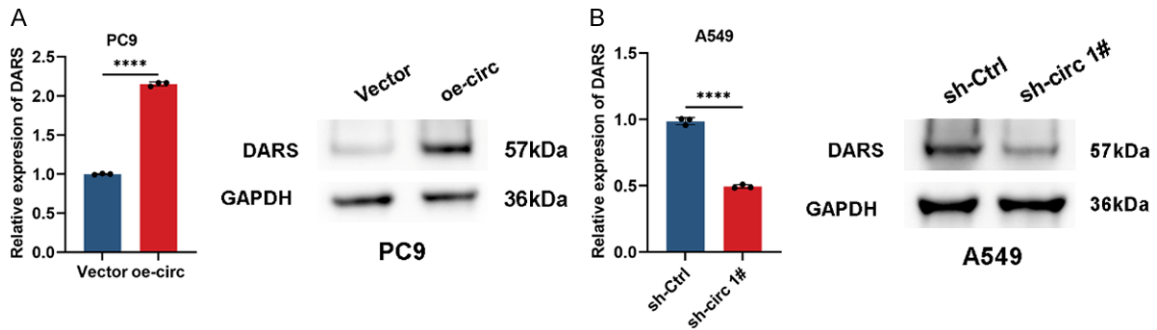
- adenocarcinoma. *J Cell Mol Med* 2021; 25: 9199-9213.
- [29] Yu F, Zhao X, Li M and Meng M. SLITRK6 promotes the progression of lung adenocarcinoma by regulating PI3K/AKT/mTOR signaling and Warburg effect. *Apoptosis* 2023; 28: 1216-1225.
- [30] Li K, Quan L, Huang F, Li Y and Shen Z. ADAM12 promotes the resistance of lung adenocarcinoma cells to EGFR-TKI and regulates the immune microenvironment by activating PI3K/Akt/mTOR and RAS signaling pathways. *Int Immunopharmacol* 2023; 122: 110580.
- [31] Chen T, Yang Z, Liu C, Wang L, Yang J, Chen L and Li W. Circ_0078767 suppresses non-small-cell lung cancer by protecting RASSF1A expression via sponging miR-330-3p. *Cell Prolif* 2019; 52: e12548.
- [32] Zhao J, Li L, Wang Q, Han H, Zhan Q and Xu M. CircRNA expression profile in early-stage lung adenocarcinoma patients. *Cell Physiol Biochem* 2017; 44: 2138-2146.
- [33] Li B, Zhu L, Lu C, Wang C, Wang H, Jin H, Ma X, Cheng Z, Yu C, Wang S, Zuo Q, Zhou Y, Wang J, Yang C, Lv Y, Jiang L and Qin W. circNDUFB2 inhibits non-small cell lung cancer progression via destabilizing IGF2BPs and activating anti-tumor immunity. *Nat Commun* 2021; 12: 295.
- [34] Dudekula DB, Panda AC, Grammatikakis I, De S, Abdelmohsen K and Gorospe M. CircInteractome: a web tool for exploring circular RNAs and their interacting proteins and microRNAs. *RNA Biol* 2016; 13: 34-42.
- [35] Liu M, Wang Q, Shen J, Yang BB and Ding X. Circbank: a comprehensive database for circRNA with standard nomenclature. *RNA Biol* 2019; 16: 899-905.
- [36] Li JH, Liu S, Zhou H, Qu LH and Yang JH. starBase v2.0: decoding miRNA-ceRNA, miRNA-ncRNA and protein-RNA interaction networks from large-scale CLIP-Seq data. *Nucleic Acids Res* 2014; 42: D92-D97.
- [37] McGeary SE, Lin KS, Shi CY, Pham TM, Bisaria N, Kelley GM and Bartel DP. The biochemical basis of microRNA targeting efficacy. *Science* 2019; 366: eaav1741.
- [38] Huang HY, Lin YC, Cui S, Huang Y, Tang Y, Xu J, Bao J, Li Y, Wen J, Zuo H, Wang W, Li J, Ni J, Ruan Y, Li L, Chen Y, Xie Y, Zhu Z, Cai X, Chen X, Yao L, Chen Y, Luo Y, LuXu S, Luo M, Chiu CM, Ma K, Zhu L, Cheng GJ, Bai C, Chiang YC, Wang L, Wei F, Lee TY and Huang HD. miRTarBase update 2022: an informative resource for experimentally validated miRNA-target interactions. *Nucleic Acids Res* 2022; 50: D222-D230.
- [39] Sang Y, Chen B, Song X, Li Y, Liang Y, Han D, Zhang N, Zhang H, Liu Y, Chen T, Li C, Wang L, Zhao W and Yang Q. circRNA_0025202 regulates tamoxifen sensitivity and tumor progression via regulating the miR-182-5p/FOXO3a axis in breast cancer. *Mol Ther* 2021; 29: 3525-3527.
- [40] Sanchez-Vega F, Mina M, Armenia J, Chatila WK, Luna A, La KC, Dimitriadoy S, Liu DL, Kantheti HS, Saghafinia S, Chakravarty D, Daian F, Gao Q, Bailey MH, Liang WW, Foltz SM, Shmulevich I, Ding L, Heins Z, Ochoa A, Gross B, Gao J, Zhang H, Kundra R, Kandath C, Bahceci I, Dervishi L, Dogrusoz U, Zhou W, Shen H, Laird PW, Way GP, Greene CS, Liang H, Xiao Y, Wang C, Iavarone A, Berger AH, Bivona TG, Lazar AJ, Hammer GD, Giordano T, Kwong LN, McArthur G, Huang C, Tward AD, Frederick MJ, McCormick F and Meyerson M; Cancer Genome Atlas Research Network; Van Allen EM, Cherniack AD, Ciriello G, Sander C and Schultz N. Oncogenic signaling pathways in the cancer genome atlas. *Cell* 2018; 173: 321-337, e10.
- [41] Li F, Wu T, Xu Y, Dong Q, Xiao J, Xu Y, Li Q, Zhang C, Gao J, Liu L, Hu X, Huang J, Li X and Zhang Y. A comprehensive overview of oncogenic pathways in human cancer. *Brief Bioinform* 2020; 21: 957-969.
- [42] Siegel RL, Miller KD and Jemal A. Cancer statistics, 2019. *CA Cancer J Clin* 2019; 69: 7-34.
- [43] Shang Q, Yang Z, Jia R and Ge S. The novel roles of circRNAs in human cancer. *Mol Cancer* 2019; 18: 6.
- [44] Wang R, Liu H, Dong M, Huang D and Yi J. Exosomal hsa_circ_0000519 modulates the NSCLC cell growth and metastasis via miR-1258/RHOV axis. *Open Med (Wars)* 2022; 17: 826-840.
- [45] Li X, Yang L and Chen LL. The biogenesis, functions, and challenges of circular RNAs. *Mol Cell* 2018; 71: 428-442.
- [46] Liu Y, Ao X, Yu W, Zhang Y and Wang J. Biogenesis, functions, and clinical implications of circular RNAs in non-small cell lung cancer. *Mol Ther Nucleic Acids* 2021; 27: 50-72.
- [47] Luo Z, Rong Z, Zhang J, Zhu Z, Yu Z, Li T, Fu Z, Qiu Z and Huang C. Circular RNA circCCDC9 acts as a miR-6792-3p sponge to suppress the progression of gastric cancer through regulating CAV1 expression. *Mol Cancer* 2020; 19: 86.
- [48] Zhang N, Nan A, Chen L, Li X, Jia Y, Qiu M, Dai X, Zhou H, Zhu J, Zhang H and Jiang Y. Circular RNA circSATB2 promotes progression of non-small cell lung cancer cells. *Mol Cancer* 2020; 19: 101.
- [49] Yu C, Cheng Z, Cui S, Mao X, Li B, Fu Y, Wang H, Jin H, Ye Q, Zhao X, Jiang L and Qin W. circFOXM1 promotes proliferation of non-small cell lung carcinoma cells by acting as a ceRNA to upregulate FAM83D. *J Exp Clin Cancer Res* 2020; 39: 55.

hsa_circ_0000519 promotes lung adenocarcinoma progression

- [50] Liu Y, Tang H, Zhang Y, Wang Q, Li S, Wang Z and Shi X. Circular RNA hsa_circ_0000519 contributes to angiogenesis and tumor progression in hepatocellular carcinoma through the miR-1296/E2F7 axis. *Hum Cell* 2023; 36: 738-751.
- [51] Novoa EM and Ribas de Pouplana L. Speeding with control: codon usage, tRNAs, and ribosomes. *Trends Genet* 2012; 28: 574-581.
- [52] Xue C, Li G, Lu J and Li L. Crosstalk between circRNAs and the PI3K/AKT signaling pathway in cancer progression. *Signal Transduct Target Ther* 2021; 6: 400.
- [53] Hoxhaj G and Manning BD. The PI3K-AKT network at the interface of oncogenic signalling and cancer metabolism. *Nat Rev Cancer* 2020; 20: 74-88.
- [54] Yang T, Shen P, Chen Q, Wu P, Yuan H, Ge W, Meng L, Huang X, Fu Y, Zhang Y, Hu W, Miao Y, Lu Z and Jiang K. FUS-induced circRHOBTB3 facilitates cell proliferation via miR-600/NACC1 mediated autophagy response in pancreatic ductal adenocarcinoma. *J Exp Clin Cancer Res* 2021; 40: 261.
- [55] Wang X, Li R, Feng L, Wang J, Qi Q, Wei W and Yu Z. Hsa_circ_0001666 promotes non-small cell lung cancer migration and invasion through miR-1184/miR-548I/AGO1 axis. *Mol Ther Oncolytics* 2022; 24: 597-611.

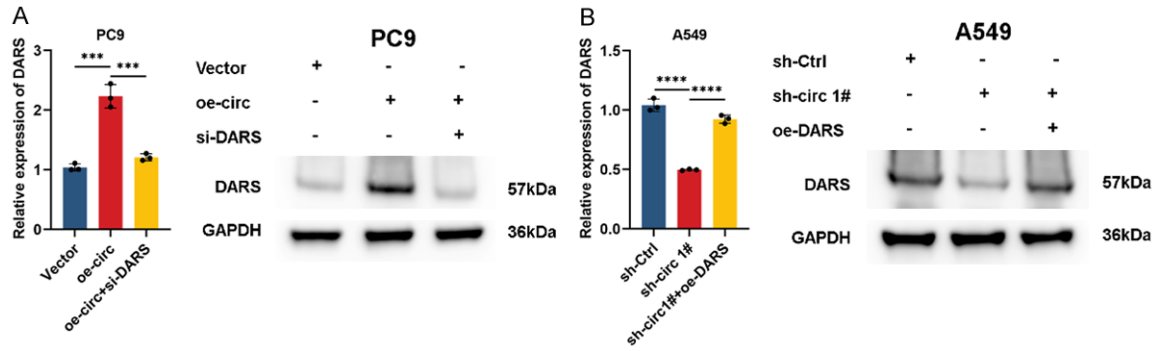


Supplementary Figure 1. The relative expression of hsa-miR-1296-5p was compared between A549 cell lines transfected with mimics NC or mimics of hsa-miR-1296-5p (A), and PC9 cell lines transfected with inhibitor NC and hsa-miR-1296-5p inhibitor (B).

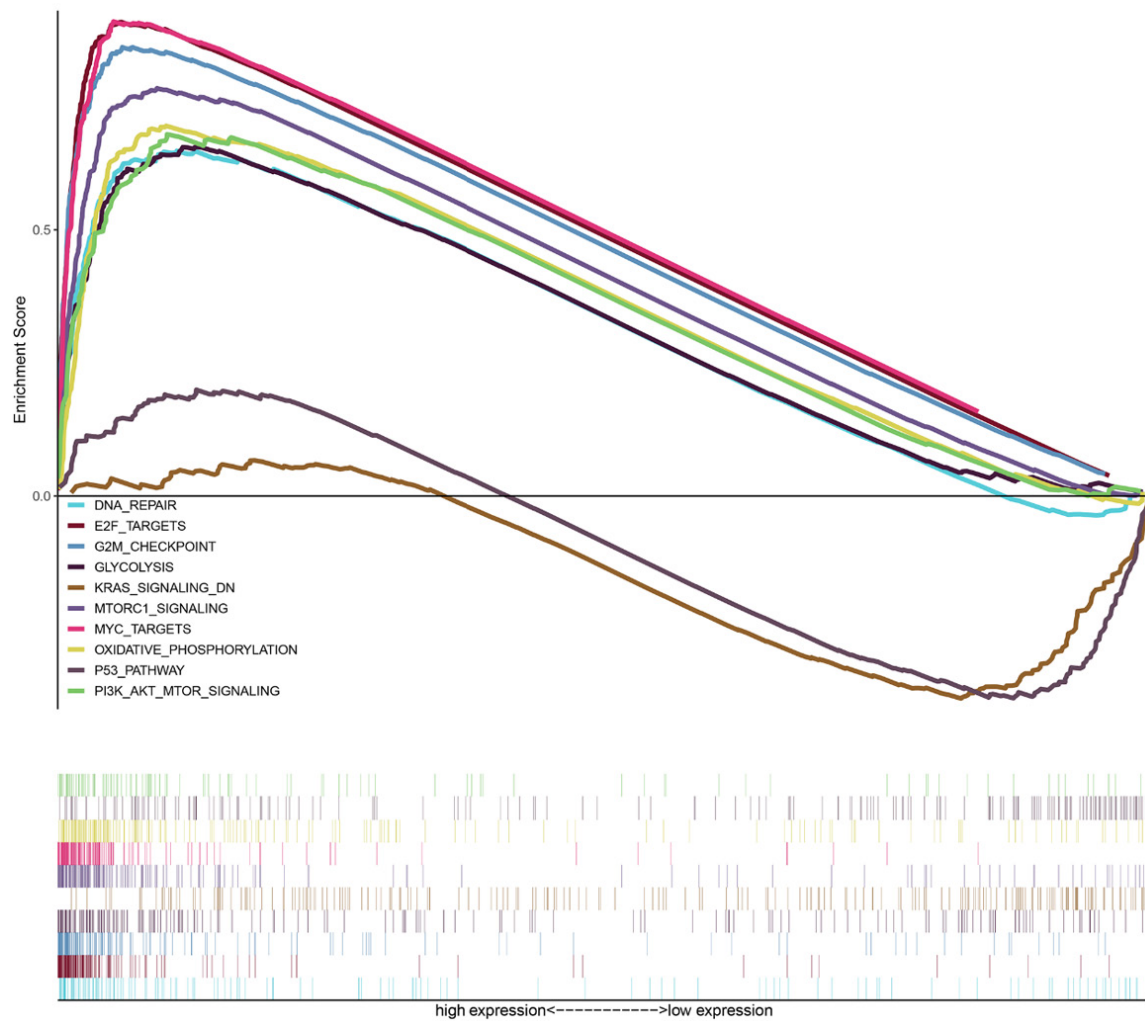


Supplementary Figure 2. The expression of DARS at mRNA and protein levels in PC9 cells transfected with vector or oe-circ (A) and A549 cell lines transfected with sh-Ctrl or sh-circ 1# (B).

hsa_circ_0000519 promotes lung adenocarcinoma progression



Supplementary Figure 3. The mRNA and protein expression levels of DARS in PC9 (A) and A549 (B) cell lines transfected with indicated plasmids.



Supplementary Figure 4. Representative cancer-related pathways enriched by GSEA.